Escuela de Caminos
Escuela Técnica Superior de Ingenieros de Caminos, Canales y Puertos
UPC BARCELONATECH

Numerical modeling of debris flows. Application to Rebaixader (Pyrenees) and Mocoa (Colombia)

MASTER FINAL THESIS

Final Thesis developed by:
Laura Isabel Molano Correa

Directed by:
Marcel Hürlimann
Vicente Medina

Master in:
Geotechnical Engineering with Specialization in Geotechnics

Barcelona, **June 2023**

Department of Civil & Environmental Engineering

Table of Contents

Abstract ***2***

Resumen ***3***

1. Introduction ***4***

1.1 Debris-flows Modeling **6**

1.1.1 Review of Existing Numerical Models 6

1.1.2 Flow Resistance Laws 9

1.2 Research Objectives **11**

2. Study Areas and Events Description ***12***

2.1 Mocoa Site **12**

2.1.1 General Characteristics of Mocoa 12

2.1.2 Previous Studies and Data Collection 16

2.2 Rebaixader Site **19**

2.2.1 Monitoring System 20

2.2.2 Description of Monitoring Data 22

3. Methodology ***24***

3.1 Description of FLATModel **24**

3.1.1 Initial Conditions and Parameters 25

3.1.2 Calibration and validation model with historical events 27

3.2 Analytical methodology of boulders transport applied to Rebaixader **30**

3.2.1 Single Rigid Block Model on an Inclined Plane 30

3.2.2 Impact by Hydrodynamic Force 31

4. Results and Discussion ***33***

4.1 Back-analysis of the 2017 Debris Flow in Mocoa **33**

4.2 Back-analysis of the 2020 Debris Flow in Rebaixader **38**

4.3 Analytical Application of Impact and Transport of Boulders **44**

4.3.1 General Aspects 44

4.3.2 Application to Rebaixader Site 45

5. Conclusions ***50***

References ***52***

Annexes ***55***

Abstract

Debris flows are one of the most hazardous geomorphological processes in mountain areas with complex behavior due to the high flow velocity, long run-out, and destructive power. The present assessment is based on numerical modeling to reproduce historical events and to predict the characteristics of a future one. Two debris flows events have been evaluated, one occurred in the Northern Andes Mountain range (Colombia), while the other event occurred in the Central Pyrenees (Spain). The back-analysis was applied to calibrate and validate simulation results for each debris flow caused by a set of parameters related to the mountain environment conditions.

In this study, the analysis of the simulations is developed by the 2D finite volume code FLATModel. Although different flow resistance laws were integrated in the numerical code, we will be comparing Bingham, and Voellmy with and without entrainment. The basal entrainment from erodible beds was evaluated, the simulation runs incorporating the Voellmy with entrainment model into FLATModel. The calibration stage involves making simplifications and proper assumptions to obtain adequate results based on historical and field-measured and monitoring data of the events. The back-analysis has been completed to find the rheological parameters which can reproduce the reference results.

In order to study debris flows dynamics, numerical modeling of two historical events was performed. Simulating Voellmy with entrainment offered satisfactory results regarding the flow path and total volume for both cases. Thus, the outcome of applying the basal entrainment provides the right agreement with field observations. The final volume is sensitive to the parameter φ_{ent}, but the impact and transport capacity is influenced by the local terrain slope and flow velocity. The concept of the critical radius is introduced to describe the areas where the flow develops a more destructive capacity and can mobilize a larger boulder size. The present study shows that in spite of many uncertainties, debris flow modeling is a key tool for researchers to increase the understanding of flow dynamics and reduce the impacts of these natural hazards.

Keywords: Debris flows; numerical modeling; basal entrainment; transport of boulders; impact force; Rebaixader; Mocoa.

Resumen

Los flujos de detritos son uno de los procesos geomorfológicos más peligrosos de las zonas montañosas, con un comportamiento complejo debido a la alta velocidad del lujo, el largo recorrido y el poder destructivo. Para esta evaluación, se utiliza la modelación numérica para reproducir eventos históricos y predecir sus características en el futuro. Se han evaluado dos eventos de flujos de detritos, uno ocurrido en la Cordillera de los Andes del Norte (Colombia), mientras que el otro evento ocurrió en los Pirineos Centrales (España). Se aplica el análisis retrospectivo para calibrar y validar los resultados de la simulación de cada flujo de detritos, causado por un conjunto de parámetros relacionados con las condiciones ambientales de la montaña.

El análisis de las simulaciones se desarrolla mediante el código de Volumen Finito 2D FLATModel. A pesar de que el código numérico integra diferentes leyes de resistencia al flujo, se realiza la comparación de Bingham y Voellmy con y sin arrastre. Se evalúa el arrastre basal de lechos erosionables, y las simulaciones ejecutadas incorporaron el modelo Voellmy con arrastre en FLATModel. La etapa de calibración involucra hacer simplificaciones y suposiciones apropiadas para obtener resultados adecuados de los eventos basados en datos históricos medidos y monitoreados en campo. El análisis retrospectivo se ha completado para encontrar los parámetros reológicos que pueden reproducir los resultados de referencia.

Para analizar la dinámica de los flujos de detritos, se realiza el modelado numérico de dos eventos históricos. La simulación de Voellmy con arrastre ofrece resultados satisfactorios en cuanto a la trayectoria del flujo y el volumen total para ambos casos. Por lo tanto, el resultado de aplicar el arrastre basal proporciona la concordancia correcta con las observaciones de campo. El volumen final es sensible al parámetro φent, pero la capacidad de impacto y transporte está influenciada por la pendiente del terreno local y la velocidad del flujo. El concepto de radio crítico se introduce para describir las áreas donde el flujo desarrolla una capacidad más destructiva y puede movilizar un tamaño de roca más grande. El presente estudio muestra que, a pesar de existir muchas incertidumbres, la modelación de flujo de detritos es una herramienta clave para que los investigadores aumenten la comprensión de la dinámica del flujo y reduzcan los impactos de estos peligros naturales.

Palabras clave: Flujos de detritos; modelación numérica; arrastre basal; transporte de cantos rodados; fuerza de impacto; rebaixader; Mocoa.

1. Introduction

The study of debris flows remains a matter of research due to its complex behavior and great impact on geological risk management. These types of flows imply the transportation of granular solids and fine particles in a multiphase integrated by water and air. Debris flows are defined as rapid movements of saturated debris in a steep channel (Jakob & Hungr, 2005), a main feature of debris flows is the fact that they move different grain sizes of sediment including gravels to boulders (Jhonson & Rodine, 1984). Once it starts, it can be highly erosive entraining sediments that make its volume grow to size. We understand erosion as removing sediment from the channel bed, while entrainment is incorporating the eroded sediment into the debris flow (Frank, et al., 2017). For this, debris flow is a high-energy phenomenon that represents a potential hazard. In any case, the mountain environment conditions, the characteristics of the flow, and the event frequency due to regional weather, geology, morphology, and hydrology make it difficult to understand.

Debris flows are a well-known geomorphic process in the wide world, and it is considered the most active geomorphic hazard in mountain areas (García-Ruiz, et al., 2002). Two debris flow cases in different locations have been evaluated and analyzed to deepen the study of this type of hazard. One event occurred in the Northern Andes Mountain range (Colombia), while the other event occurred in the Central Pyrenees (Spain).

The first case takes place in South America, with a varied topography, where the Andes Mountains have a large extension on the continent. The Andes Mountains were formed by the subduction of the Nazca Plate under the South American Plate (Prada-Sarmiento, et al., 2019). Several fault systems such as the Mocoa-La Tebaida Fault and the Cantayaco Fault were generated in southwestern Colombia. The tectonic weakening of the local geology reflects critical conditions on basin hillslopes which are covered by erodible materials from highly weathered rocks (García-Delgado, et al., 2019). Previous events of landslides, debris flows, and mudflows were developed in the Mocoa basin triggered by the prolonged and intense rainfalls of a tropical zone. The topography of the area varies from flat to hilly to steep and the water sources have produced deep V-

shaped channels because of the high erosion rates (Prada-Sarmiento, et al., 2019). Although previous events have occurred in the Mocoa basin, the catastrophic event in 2017 has motivated the investigation of flow description and volume estimation through numerical modeling.

In contrast, the second case occurs in the Pyrenees, frequently affected by flows triggered mainly by rainstorms (Portilla, et al., 2010). Identifying several episodes in this zone incentives the investigation of the susceptibility's causes and dynamical behavior (Portilla, et al., 2010). The characteristics investigated in the Pyrenees resemble those found in the Alps (Portilla, et al., 2010), where the steepness of slopes, the high production of accumulated debris, the frequent occurrence of rainstorms, and the characteristics of some lithological outcrops stand out (García-Delgado, et al., 2019). The case under study occurred in the Rebaixader catchment in which a monitoring system detects torrential flows and collects information to compare with the models. The monitoring setup includes sensors related to in-situ measurements of initiation and flow dynamics (Hürlimann, et al., 2014).

The regions with hazard phenomena such as debris flow implement mitigation measures classified as structural and non-structural (Hübl, et al., 2009). Structural measures are divided into active or passive mitigation. Where the active one intervenes directly in the process (Hübl, et al., 2009). A very common structural mitigation measure is debris flows barriers built with concrete (Hübl, et al., 2009). The design requires the estimation of the impact force of the debris flows against the obstacle. The impact models are principally based on theoretical considerations, real-world observations, and laboratory experiments (Hübl, et al., 2009). Impact signal results from current laboratory tests investigations show a typical impact process of debris flows described by a turbulent font (Cui, et al., 2015). Moreover, the grain impact loading is random, and the impact frequency of the big grains was likely to increase with the depth (Cui, et al., 2015). The tendency is that large grains are concentrated in the surface and middle parts of the flows, but the laboratory simulations are limited by the flume size to represent the effects of big boulders (Cui, et al., 2015). Several observations conclude that the large blocks are transported by debris flows, even though the flow is turbulent, the blocks stop, and the debris is carrying them (Jhonson & Rodine, 1984).

For the mitigation of this hazard, it is essential to understand the dynamics of flows by estimating rheology or entrainment to predict the debris behavior. Numerical models have been developed to forecast the run-out distance, the impact force, and the erosive process. Each debris flow corresponds to a set of parameters that accurately represent a single event and consequently, modeling is important to predict the spatial hazard of debris flows (García-Ruiz, et al., 2002). In this study, the analysis of the simulations is developed by the 2D finite volume code FLATModel. The application of FLATModel to catchments in the Pyrenees made it possible to generate hazard maps and validate the implementation of basal entrainment (Medina, et al., 2008), (Hürlimann, et al., 2008). The field-measured data were compared with the simulation results regarding the main deposit's extension and the thickness of the final deposits (Hürlimann, et al., 2008). The evaluation of specific debris flows also provided information that described how the stop-and-go mechanism is simulated by FLATModel (Medina, et al., 2008). Considering the successful application in the Pyrenees basins, the numerical model is implemented for the first time in a catchment located in the Colombian Massif. The calibration and validation of the back-analysis for the Mocoa event have many limiting factors. The measured field data of flow depth and velocity during the event was lacking. Additionally, there is no available rheological data on the material.

1.1 Debris-flows Modeling

1.1.1 Review of Existing Numerical Models

There are many numerical models for simulating single-phase or multiple-phase flows. The approach for these models is based on the fact that future debris flows will behave comparably to those that have previously occurred (Jhonson & Rodine, 1984). The simulations with single-phase models are frequently used to predict and evaluate the behavior of an event (Medina, et al., 2008). Working with two phases implies handling separately the fluid and grains. This assumption is based on the effect of the sediment grains' interactions and in most cases, the phases remain uncoupled during all analyses (Medina, et al., 2008).

Regardless of the definition of the phases, measuring flow parameters is challenging because the material properties may change in time and space (Rickenmann, et al., 2006). Normally, the models allow more than one flow resistance law, and it can assume the density as a known parameter. Even more, it is determinant to have an accurate digital surface model because the results may improve if flow obstructions such as buildings are included (Núñez-Andrés, et al., 2019). In addition, the availability of the terrain data before and after an event can be compared to obtain the quantification of mobilized volume and erosion (Núñez-Andrés, et al., 2019).

The table below makes a comparison of some numerical models. The most recent codes are trying to incorporate the use of multiple-phase flows and the simulation of entrainment. The latter process should be considered in debris flow simulations because can strongly increase the event's volume, runout distance, and impact force (Baggio, et al., 2021).

Table 1. Summary table of some available numerical models.

NAME (REFERENCES)	NUMBER OF PHASES	FLOW RESISTANCE LAW	SIMULATION OF ENTRAINMENT	NUMERICAL SCHEME	COST
D-CLAW (George & Iverson, 2014)	Biphasic	Turbulent-Coulomb		Finite Volume	Free
DFEM (Naef, et al., 2006)	Monophasic	Bingham, dilatant, turbulent and Coulomb	X	Finite Element	Free
FLATModel (Medina, et al., 2008)	Monophasic	Manning, Coulomb, Voellmy, Bingham, Herschel-Bulkley	X	Finite Volume	Free
FLO-2D (Cesca & D'Agostino, 2008)	Monophasic	Turbulent-Coulomb-viscous	X	Finite Difference	Commercial
Morpho2DH (Takebayashi & Fujita, 2020)	Monophasic	Turbulent, Coulomb, and creep	X	Finite Element	Free
RAMMS (Frank, et al., 2015)	Monophasic	Voellmy	X	Finite Difference	Commercial
R. AVAFLOW (Baggio, et al., 2021)	Mono-, bi- and triphasic	Bingham plastic (liquid phase), viscous Coulomb or visco-plastic (coarse solid phase)	X	Finite Difference	Free
RIVERFLOW2D (Pasculli, et al., 2021)	Monophasic	7 rheological models		Finite Volume	Commercial
TRENT-2D (Stancanelli & Foti, 2015)	Biphasic	Voellmy	X	Finite Volume	Free

1.1.2 Flow Resistance Laws

The physical models involved in debris flow simulation are not the same for all the events because each one is improved under certain hypotheses, and it is adapted to solve a specific scenario (Medina, et al., 2008). Therefore, it is necessary to define the flow resistance law of the model and calibrated its rheological parameters considering the constitutive equation of the mixture (Medina, et al., 2008). There is a complexity to simulate real mixtures with the current constitutive approaches because the computational models demand multiple topographic details and parameter calibration. Also, the models initially considered high fluidity as a property because of the significant amount of water content found in the mixture. However, there was no field evidence of the required quantity of water to reach the fluidization of the debris flow (Jhonson & Rodine, 1984). Thus, the development of numerical models involved making simplifications and proper assumptions to obtain adequate results. Most of the current numerical models provide the output of the debris flows front velocity and flow depth. Previous investigations aim to quantify the risk with a numerical analysis approach because of the difficulties entailed in the field of measuring flow velocity for estimating impact forces (Jakob, et al., 2012). The risk quantification can be expressed as a function of vulnerability which is related to the consequences of natural hazards, generally measured in terms of damages or losses (Fuchs, et al., 2007).

The mathematical approach to describing debris flows considers the presence of yield strength and shear stress (Jhonson & Rodine, 1984). In this sense, the models propose the conservation of momentum and mass, even more, all of them establish the rheological properties that fit with the flow dynamic (Jhonson & Rodine, 1984). The most common flow resistance laws to describe rheological behavior are Manning, Coulomb, Bingham, Herschel-Bulkley, quadratic rheology, and Voellmy. However, this study delimitated the simulation analyses into Bingham rheology and the Voellmy fluid model to estimate the debris flow dynamics. Likewise, it is important that no matter how robust a numerical model is formulated, a wrong selection of the flow resistance law will result in an erroneous outcome (Arattano, et al., 2006).

The Bingham model is a mechanical model that combines plastic and viscous attributes. This resistance law defines a single phase in movement that continue rigid or elastic, while the deviatoric stresses do not exceed the plastic yield strength (Iverson, 1997). Despite this, the Bingham model has a lot of limitations on model debris flows because it assumes the movement of the material in the upper layer thus it does not contribute to the effect of the sediment grains interactions (Iverson, 1997). The velocity profile of the flows was developed by defining the basal shear stress (τ_b) by (Medina, et al., 2008):

$$\tau_b = \tau_0 + \mu_m \left(\frac{dV}{dz}\right) \tag{1}$$

Where, τ_0 is the threshold basal shear stress to start the motion, μ_m the Bingham viscosity, and dV/dz, is the velocity gradient. In this case, the Bingham rheology should be integrated to obtain the bed shear stresses as a function of the mean velocity, $\bar{v}$, and depth, d. After the depth integration is done, we get (Medina Iglesias, 2011):

$$\bar{\upsilon} = \frac{\tau_0\, d}{3\mu_m}\left(1 - 1.5\frac{\tau_b}{\tau_0} + 0.5\left(\frac{\tau_b}{\tau_0}\right)^3\right) \tag{2}$$

On the other hand, the Voellmy approach refers to an empirical mathematical expression for granular friction. This law appears to be a very common model to the back analyses on debris flows because it includes the slope to start the motion as an input parameter independent of flow height (Medina Iglesias, 2011). The expression of equation 3 from the Voellmy model was implemented into the numerical modeling as the basal shear stress (Medina, et al., 2008):

$$\tau_b = g\rho\left(h\cos(\theta)\tan(\varphi) + \left(\frac{V}{C_z}\right)^2\right) \tag{3}$$

Where g is the gravity, ρ the flow density, h the flow depth, θ the angle defined by the horizontal plane and the flow direction, φ the internal friction angle, V is the mean velocity of the flow, and Cz the Chezy coefficient.

1.2 Research Objectives

The main goal of this research is to investigate and describe the debris flow dynamics of Rebaixader´s event in 2020 and Mocoa's event in 2017 through the simulations incorporating the effect of basal entrainment into the 2D finite volume code FLATModel, based on the historical and field-measured data of events.

Specific objectives:

a) Review the state of the art in numerical debris-flow modeling identifying the influence of the flow resistance laws.

b) Analyze the available information on the events associated with monitoring data and field measurements/observations published in previous studies.

c) Develop the back-analysis of the event in the Rebaixader (Pyrenees) and Mocoa (Colombia) applying different Digital Elevation Models (DEMs) and parameters to calibrate and validate the model implemented into FLATModel.

2. Study Areas and Events Description

2.1 Mocoa Site

2.1.1 General Characteristics of Mocoa

Mocoa is the capital of the department of Putumayo in Colombia. The catchment is located in the Piedmont between the Amazon plains and the Colombian Massif as seen in Figure 1. The study area is around 46.8 km^2 where the micro-basins of the San Antonio, the Taruca, and Taruquita creeks and the Sangoyo and Carmen rivers are located (Ruiz, et al., 2018). Although the main alluvial fan extends around over 15 km^2 that receives the eroded material of the basins of the San Antonio, the Taruca, and Taruquita creeks (Ruiz, et al., 2018). The catchment is the boundary by the Mocoa-La Tebaida fault and the Catayaco fault which are thrust faults but only the first one shows signs of constant neotectonics activity (Prada-Sarmiento, et al., 2019). Moreover, the basin is divided into three geological zones associated with the presence of faults as described in Figure 1.

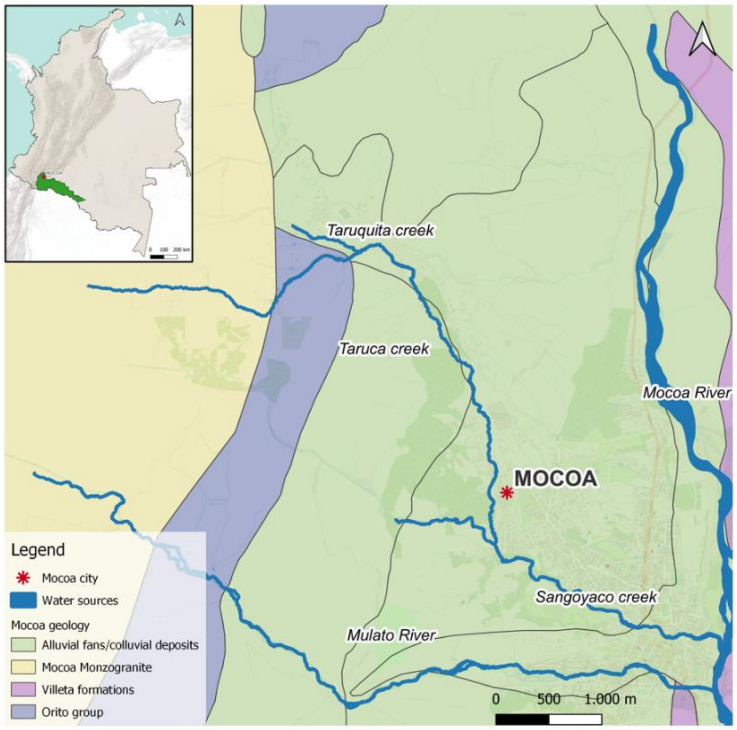

Figure 1. The location of Mocoa in Colombia. Geological map and water sources of the study area.

The block fall zone is associated with the highest gradient in Taruca Creek where the average is around 38%=20.7°. In Figure 2 the upper part of the basin corresponds to the highest terrain slopes between 50° and 70°, it is composed of the geological unit of highly fractured Mocoa Monzogranite with spherical weathering (Prada-Sarmiento, et al., 2019). In the middle zone are mainly the geological units of the Orito and Pepino formations. The Orito group are mudstone, lithic sandstone, and intercalations of ferruginous conglomerates (Gómez & Montes, 2020). While the Pepino formations are intercalations of layers of conglomerates, conglomeratic lithic sandstones, and claystone (Gómez & Montes, 2020). The third zone in the lower part corresponds to alluvial fans and colluvial deposits, largely from the Rumiyaco and Villeta formations (Gómez & Montes, 2020). The entrance of the urban area is placed in the third zone where the basin fan develops with a terrain slope angle of less than 7°. Regarding the morphology of the mountains, the study area has variable conditions from flat to hilly to steep. After the confluence of Taruca Creek with Taruquita Creek, its alluvial fan starts developing with less gradient reaching values of 8.2%=4.7°. The geomorphological features are similar among Taruca and Taruquita creeks, but the mass removal process caused by detonation or reactivation in the Taruquita Creek has been in a smaller area than in Taruca Creek (Medina, et al., 2017). For this reason, it is expected that Taruquita Creek provided less eroded material to the final deposit. Figure 2 presents the terrain slope angle map in the interest extension and three checkpoints to describe flow characteristics.

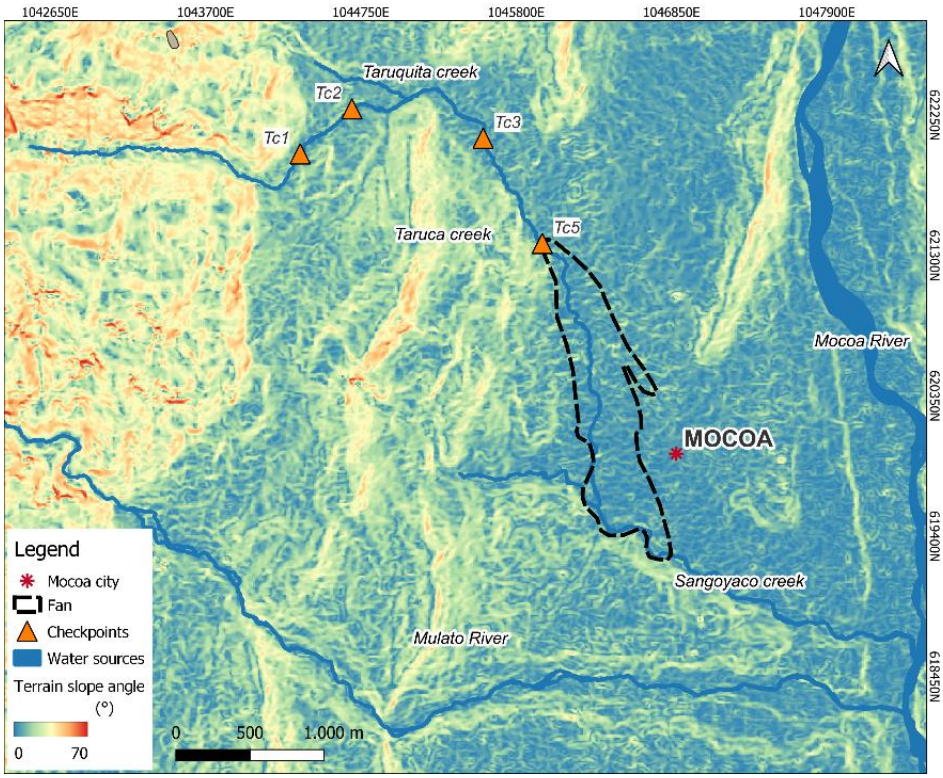

Figure 2. Terrain slope map derivated from a 5m resolution Digital Elevation Model (DEM) with triangle marks to denote the checkpoints.

Mocoa City has a monthly multiannual precipitation (MMA) distribution dominated by two regimes: the rainy season (La Niña event) and the dry season (El Niño event). Nevertheless, the regimes are related to the weather that depends on sea temperature, winds, pressure, and other oceanic and atmospheric variables. During the rainy season, the MMA is over 300 mm which covers the months between March and August, while the dry season is usually between October to February with an MMA of less than 250 mm (García-Delgado, et al., 2019). In Mocoa, there are 6 stations installed by the Institute of Hydrology, Meteorology, and Environmental Studies (IDEAM) to measure and record precipitation. The month with the highest precipitation is in June with an average value of 531 mm/month but the transition months are February and March when rainstorms intensify (Ruiz, et al., 2018).

Precipitation is a process associated with wearing a way of soil and it raises the susceptibility to landslides and infiltration (Medina, et al., 2017). The Putumayo location has a higher degree of erosion due to the seasonal rain and the proximity to the Amazonian region. In consequence, this zone presents a higher fracturing degree attributed to tectonic weakening and intensify by climate conditions (Medina, et al., 2017). Outcrops of Monzogranite are unstable and promote the formation of sedimental deposits and frequent mass movements. The Monzogranite of Mocoa has compositionally variations to granite, granodiorite, quartz monzonite, quartz diorite, and monzodiorite (Medina, et al., 2017). Figure 3 presents granodiorite outcrops heavily fractured and weathered upstream of Taruca Creek. The bed material corresponds to fractured Monzogranite, which reaches an effective friction angle of around 30° (Medina, et al., 2017).

Figure 3. Outcrops of granodiorite were observed during field visits at Taruca Creek (Pontificia Universidad Javeriana, 2017).

2.1.2 Previous Studies and Data Collection

Based on the historical archives of Mocoa, the fluvial-torrential events date from the years 1947 and 1960 for the Mulato River and the Taruca Creek respectively, but the deposits under the urban area are even older (Medina, et al., 2017). A large part of the Taruca and Taruquita Creeks fan is placed in the urban area. The magnitude of the damage in the 1960 debris flow event is not comparable with the 2017 event due to population growth. Besides, there have been geomorphological alterations causing elongated V-shaped basins that suggested active valleys where bedrock incisions are rewarded by several landslides (García-Delgado, et al., 2019). The dynamics of both creeks are controlled by fluvial-torrential events with entraining material and damming where the channel narrows or is obstructed by active mass movements (Medina, et al., 2017). The catastrophe that occurred on March 31, 2017, was caused by subsequent mass movements in the Mocoa basin. The debris flow events were triggered by four days of high-intensity rainstorms during the rainy season (Prada-Sarmiento, et al., 2019).

The Colombian Geological Service (SGC) has developed projects to classify mass movements, record observations, and estimate the volumes contributed to drainage. Based on the study carried out by Medina, et al., (2017), a total of 629 mass movements were cartographically identified. The use of the photointerpretation technique allowed identify 179 mass movements in the Taruca, and Taruquita creeks of which 84 of them provided eroded material to the flow (Medina, et al., 2017). These 84 mass movements correspond to debris flows because its deposit matrix consists of boulders and angular monzogranite blocks (Medina, et al., 2017). In addition, Medina et al. (2017) estimated that subsequent debris flows events added to the drainage around 187831 m^3 to reach an approximate total volume of $2.25x10^6$ m^3 in the fan. Subsequently, the volume in the fan was updated to $3x10^6$ m^3 and the eroded material represents 13% of the total debris volume (Medina, et al., 2017). The flow height was described in the study of Medina, et al., (2017) (see Figure 25), where it is observed that the highest flow depth was about 13 m in the channel of Taruca and Taruquita creeks. It should be noted that these zones are related to the points of the greatest slopes change of the torrent (Medina, et al., 2017). In the Medina, et al., (2017) report was concluded that the Taruca and Taruquita mass movements gain volume rapidly, at first removing the organic

material and then the water and sediment volume increased, which led to a rise in the erosion capability and obstructions were overcome. Regarding the dynamics of the flow and the material accumulation, the transport of boulders may hinder free movement and causes damming. The obstructions represent energy accumulation which results in higher velocities when the material is released.

One year later Ruiz, et al., (2018) with the SGC developed a project for hydraulic calibration, the geomorphometric of the micro-basins, and mass movement hazard mapping. In contrast to the previous study Ruiz, et al., (2018) used FLO2D to simulate the 2017 event and they compared their flow velocities outcomes with the empirical ones described in Medina, et al., (2017). The numerical modeling discharge results for the basin established by the San Antonio, Taruca, and Taruquita creeks were in a range of 55 m^3/s to 220 m^3/s (Ruiz, et al., 2018). Likewise, the velocities fluctuate between 2.78 m/s and 17.22 m/s with a range flow depth of 1.3m to 11.7m (Ruiz, et al., 2018). The simulate mobilized volume was 2123583 m^3 with a solids concentration of 45% (Ruiz, et al., 2018). Nevertheless, the study stands out that the uncertainties of the section results (see Table 5) are significant because of the complex geological-structural conditions (Ruiz, et al., 2018). Even more, the lack of instrumentation in the micro-basin does not allow us to know with certainty the behavior of the flow. In consequence, they suggest the comparison of the results focuses on the affected urban areas (Ruiz, et al., 2018). Other authors (Pontificia Universidad Javeriana, 2017), (Prada-Sarmiento, et al., 2019), (García-Delgado, et al., 2019) relied on the SGC projects to describe and increase the understanding of the triggering factors, of transport, and deposit of mass movements.

Additionally, the early warning system (EWS) was designed by Pontificia Universidad Javeriana after the event in 2017 and was developed through field technician visits supported by the National Unit for Disaster Risk Management (UNGRD). The EWS had a period of research and numerical modeling through software, where the academy and the UNGRD generated a baseline to make public decisions. Monitoring equipment to measure hydraulic and meteorological conditions were implemented. Moreover, an alert communication system was incorporated which is

integrated by sirens, local communication equipment, and data storage providing management real-time data. (Pontificia Universidad Javeriana, 2017)

During the field visits, they observed that the deposits in the upper part of the Taruca basin are thin with the Monzogranite outcrops, while the accumulation increased in the lower part of the Taruca and Taruquita creeks (Pontificia Universidad Javeriana, 2017). The thickness of the accumulation can reach up to 4-5m and they identified different mass movements which stand out: the Monzogranite rockfall and translational landslides (Pontificia Universidad Javeriana, 2017). The change in rock composition from igneous domain to sedimentary added to the slope change, enables material to deposit as shown in Figure 4. In contrast, Figure 5 presents the lower level where the matrix consisted of size grains of medium sand to coarse sand with angular shapes (Pontificia Universidad Javeriana, 2017). Also, they noted fragments of diameters from 0.2m to 3m of granodiorite and granite with a maximum percentage of clay of 20% (Pontificia Universidad Javeriana, 2017).

Figure 4. Deposit caused by torrential flow at Taruca Creek (Pontificia Universidad Javeriana, 2017).

Figure 5. Deposit distribution downstream of the Taruca and Taruquita confluence (Pontificia Universidad Javeriana, 2017).

2.2 Rebaixader Site

The Rebaixader site is a small catchment located in the Central Pyrenees, which has been affected by many debris flow events due to high mountain morphology. The drainage basin covers a total area of 0.5 km^2, where the bedrock is composed of Paleozoic metamorphic rocks, and the material that covers the bedrock is colluvium and granular glacial deposits (Núñez-Andrés, et al., 2019). The basin is divided into four zones of analysis as shown in Figure 6: scarp, funnel, channel, and fan. The scarp includes the entire initiation area where there is unlimited sediment availability with the highest slopes, in a range of 30° to 60°. Then downstream, the funnel is located, and it presents a large amount of accumulated sediment due to the channeling of the flow. This zone has a mean slope angle of about 30° before arriving at the channel, and it remains around 30° across to channel. The last zone is the fan with the lowest slopes between 15° and 20°, where the material is deposited or sometimes the debris drains into the Noguera Ribagorçana River.

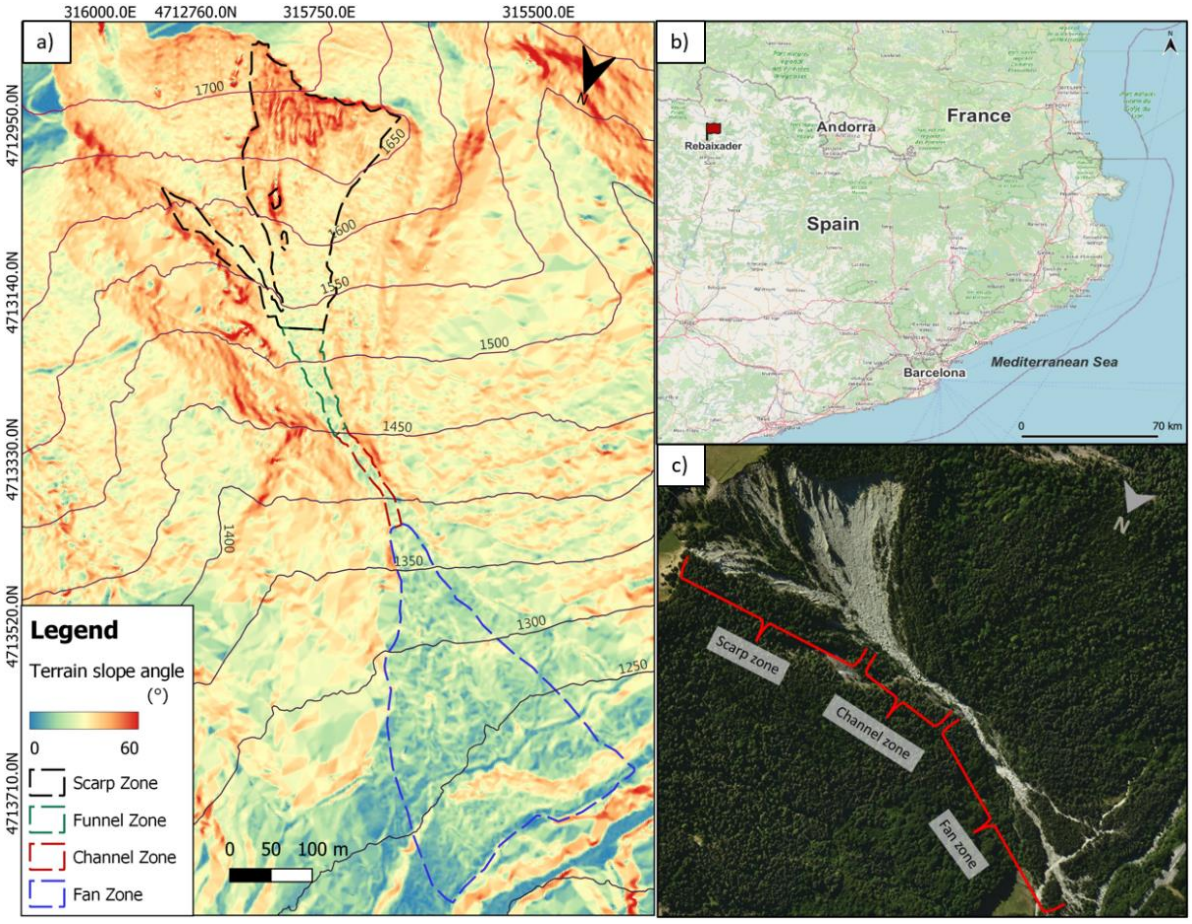

Figure 6. The Rebaixader site a) Slope angle map based on the ICGC data with dashed polygons to indicate the different morphologic domains (contour lines: 50m; raster resolution: 1x1m). b) Location of the Rebaixader site. c) Satellite image with the four morphologic domains.

2.2.1 Monitoring System

In the summer of 2009, a monitoring system was installed in Rebaixader, and over the years it has been developed and improved. The benefit of implementing a monitoring system in a site where there are no countermeasures is to allow the study of torrential activity. Currently, the system consists of four different stations to record information in the initiation zone and the channel. Two infiltration stations are located in the scarp to identify the initiation of the movement (Hürlimann, et al., 2014). Another station is the meteorological station. Finally, the flow behavior is monitored by the devices placed along about 175 m in the active channel. There are three types of monitoring devices: the geophones that measure vibrations, the ultrasonic and radar sensors to

record the flow height, and the video camera to confirm the facts (Figure 7). The devices mentioned above are wired sensor networks, although other types of sensors with wireless communication have recently been installed. In 2009 were installed the geophones and the ultrasonic device (US) which are connected by electrical wires with a Campbell Scientific CR1000 datalogger (Hürlimann, et al., 2014). Installing geophones along the channel was a success because the devices record information from a place separated from the torrent without risk of damage.

Previous antecedents showed that most events were triggered by short high-intensity rainstorms during the summer, but also during spring due to the melting of snow (Hürlimann, et al., 2014). The interpretation of the data is supported with ultrasonic and radar measures and using a camera to clarify details. The sensors switch to "event" mode if the defined threshold is exceeded, for instance, the geophones threshold is defined by 20 IMP/s during three consecutive seconds (Hürlimann, et al., 2014). At this moment, the geophones record the impulse per second (IMP/s) in the datalogger internal memory. In addition, the radar and the US are measuring every second the flow depth. The distance along the channel of each sensor is listed in Table 2. Moreover, the study area is monitored with the geomatic technique of digital photography from UAV (Unmanned Aerial Vehicle) to capture the morphologic changes. In our case, the scarp has large blocks and steep slopes that increased difficulties to generate an accurate point cloud (Núñez-Andrés, et al., 2019).

Table 2. Terrain distance of the devices. See Figure 7 for location.

SENSOR IDENTIFIER	TERRAIN DISTANCE (m)
Geophone 2 - Radar	77
Geophone 2 - US	65.9
Geophone 2 - Geophone 4	139.2

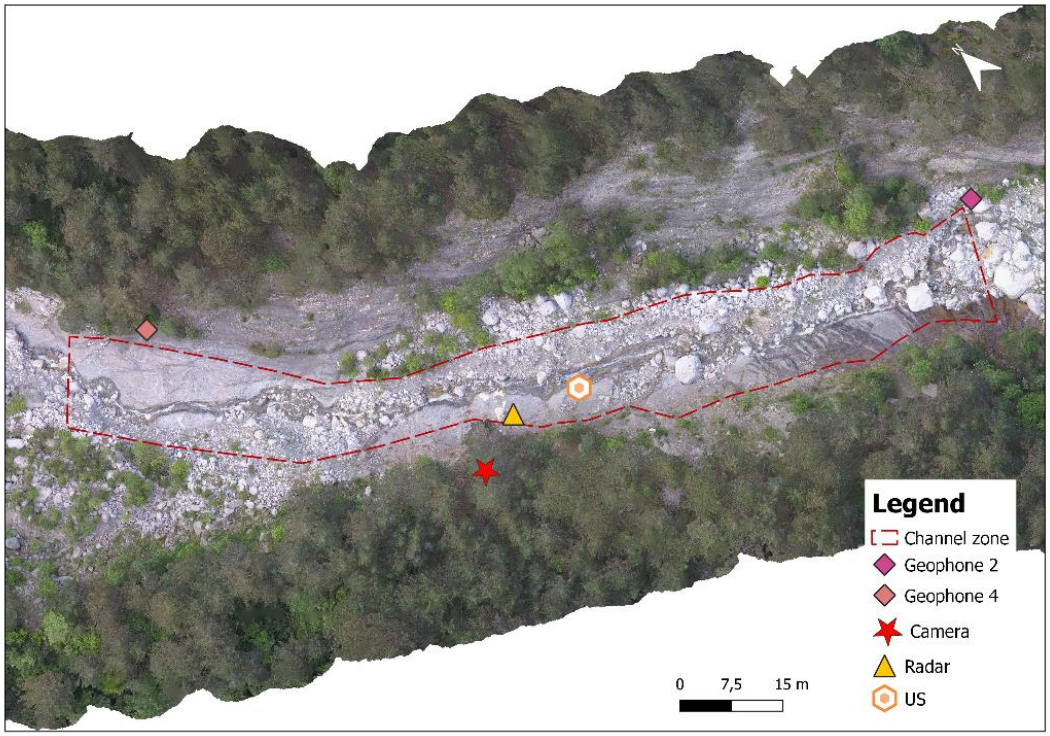

Figure 7. Instrumentation devices used in this study and installed at the channel zone for the monitoring system: two geophones, the camera, the radar, and the ultrasonic device (US).

2.2.2 Description of Monitoring Data

We select the July 2020 debris flow as a recent event due to significant data availability. The debris flow was triggered by a rainstorm, where the critical hourly rainfall was about 14.6 mm/h. This threshold fits with previous correlations made in the Rebaixader torrent, where it is suggested a value of around 15 mm/h for the summer season (Hürlimann, et al., 2014). The back-analyses of this debris flow are based on the monitored information, particularly with the sensors in the channel to describe accurately the flow dynamics.

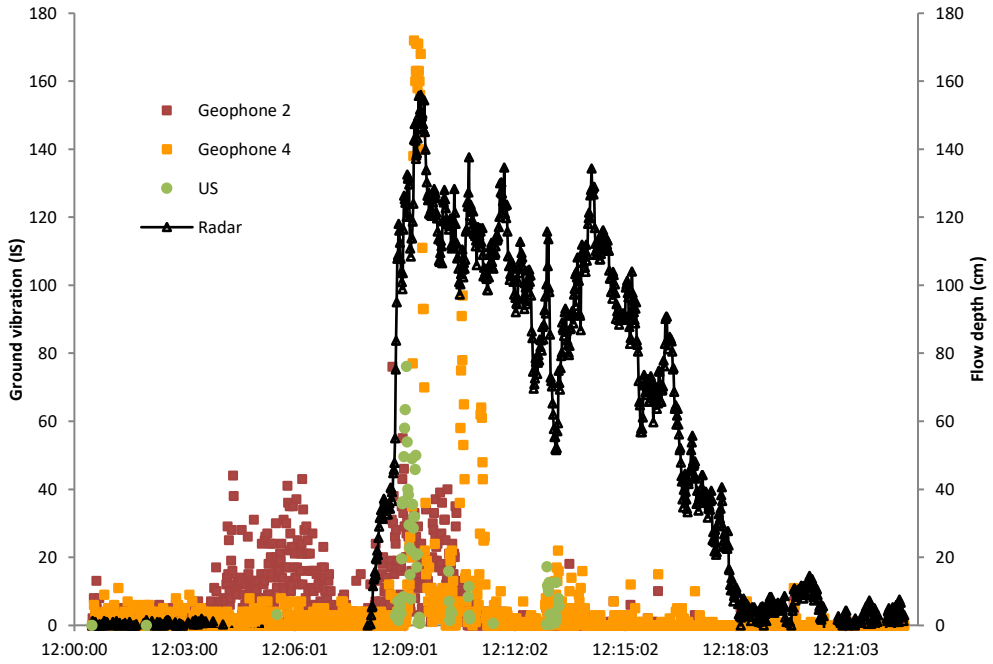

Figure 8. Monitoring data recorded for the debris flow event.

Figure 8 presents the information recorded by the monitoring system in the channel during the 2020 event. Geophones 2 and 4 measured the ground vibrations signal that was transformed and recorded by impulse per second (IS). These two devices registered the information for an analysis of the seismic data of a debris flow. The most typical feature in this type of recording is the steep front because the maximum vibration is associated with the impacts of large boulders (Hürlimann, et al., 2014). Then, the recorded data tends to a gradual decrease after the front with some additional peaks due to surges (Hürlimann, et al., 2014). This behavior is observed in Figure 8 in the IS time series registered of geophones 2 and geophones 4. The difference between the series of geophones can be because of their placement along the channel. On the other hand, Figure 8 contains the hydrograph by the measured data with the ultrasonic device (US) and the radar. The event starts at noon around 12:00:00h where the first minutes of the recording showed a minimum flow depth below 10 m. The US data appears to have intervals with small variations that are related to a sensor malfunction. However, the peak of maximum increase of flow height seems to fit at the same time of the event based on US data and radar measurements. At the channel, the volume estimate of debris flows that were mobilized is around 10000 m^3. This estimation was developed

with the monitored data considering a maximum flow depth of 1.6 m, an average front velocity of 4.1 m/s in the section of the flow-depth sensor, and the simplified approach described in Hürlimann, et al., (2014).

3. Methodology

3.1 Description of FLATModel

The simulations of this study have been realized through the numerical model of FLATModel, which is a two-dimensional model based on the finite volume method (FVM) with the Godunov Scheme (Medina, et al., 2008). This computational scheme has the advantage of handling discontinuities and large function gradients. The governing equations are based on a depth integration using the shallow water hypothesis and integrating the Navier-Stokes equations for thin 1D flows over smooth terrain (Medina, et al., 2008). The numerical approach includes the first and second derivatives of the terrain surface to become a correct description of a continuous surface (Medina, et al., 2008).

There are two ways that the model can simulate the entrainment, a static and dynamic approach. In both approaches, the entrainment occurs if the bed forces are greater than the resistance ones. The static equilibrium considers that the resultant velocity reduces because of entrainment, while with the dynamic method, the newly incorporated material is accelerated to the mean velocity of the flow (Medina, et al., 2008). FLATModel considers that flow depth is normal to the bed, so after solving the integration with the consideration of the direction and corrections about slope and curvature, the equation can be expressed by (Medina, et al., 2008):

$$\frac{\partial}{\partial t}\begin{pmatrix} h \\ hu \\ hv \end{pmatrix} + \frac{\partial}{\partial x}\begin{pmatrix} hu \\ hu^2 + g_p\frac{h^2}{2} \\ huv \end{pmatrix} + \frac{\partial}{\partial x}\begin{pmatrix} hv \\ huv \\ hu^2 + g_p\frac{h^2}{2} \end{pmatrix} = \begin{pmatrix} 0 \\ h(g_p \tan\alpha_x - S_{f_x}) \\ h(g_p \tan\alpha_y - S_{f_y}) \end{pmatrix} \quad (4)$$

Where the variables *u*, and *v* are the velocities in the respective directions *x*, *y*, and also the sub-index for indicates vector component, while g_p is the corrected gravity, S_f the energy gradient, α is the terrain surface angle, and *t* the temporal coordinate (Medina, et al., 2008).

One important incorporation was the two different approximations to simulate the effect of entrainment, as static or dynamic approach, assuming that the bed shear stress of the flow is significant to add material of the bed into the flow. The static approach considers a static equilibrium between the flow frictional forces (τ_b) and the basal resistance forces (τ_{res}) (Medina, et al., 2008). This means that entrainment is caused if the condition is accomplished: $\tau_b > \tau_{res}$. Because the forces depend on the terrain slope (θ) and the internal friction angle (φ), also this condition must be filled: $\theta > \varphi$. As a result, the velocity decreases and the flow depth should reduce to compute the effective stresses and not total stresses (Medina, et al., 2008). In contrast, the dynamic approach occurs in the same way as the static one with the difference that the new material is accelerated to the mean velocity of the flow (Medina, et al., 2008). Moreover, it should be noted that FLATModel cannot distinguish between water and sediment as two different phases.

3.1.1 Initial Conditions and Parameters

The essential inputs of FLATModel are three text files (a master file and files for hydrograph) and three ASCII raster files (DEM, initiation area, and calculation domain). The master file collects all the input parameters such as the computational time, the number of result files exported, rheological parameters, and control of entrainment among others. Regarding the raster files, an optional one is available for the incorporation of basal erosion while the values indicate the maximum depth of erosion. The raster called *topo* represents the DEM of the initial topography before the event with a known resolution. Otherwise, the file *ini_area* represents the initial volume of mobilized material, where the grid has the depth of material in motion and the rest is equal to zero. And the file *domain* is a raster to define the extent of the area that is assumed to be inundated. Specifically, it is a grid with zeros for the outside area and a value of 1 for the area of interest. Regarding basal erosion, the algorithm identifies as the main condition a high bed shear stress of the flow to add part of the bed into the flow.

The file topo with the DEM is a quantitative representation of the terrain, where elevation values are arranged in equal grid intervals in referenced horizontal and vertical directions (Saleem, et al., 2019). DEMs are key input information to computational models because their derived attributes (slope, aspect, drainage network or topographic index, etc.) allow the assessment of any process involving terrain analysis (Saleem, et al., 2019). The accurate representation of the terrain depends on the spatial information recorded which is called the DEM resolution. High-resolution DEMs are considered more reliable due to the amount of data but this involves overly calculation time-consuming. Consequently, a good simulation must find a balance between the accuracy of the outcomes and efficiency in terms of computational time (Li, et al., 2022).

As previously mentioned, the Rebaixader catchment is monitored with UAV from which the DEM is derived. The available pre-event DEM dates from 2019 are georeferenced with a coordinate reference system UTM 31N (ETRS89) and it has a resolution of 1m. This DEM is adequate for the numerical simulation because it is detailed enough, and the computational time is not excessive. On the other hand, Mocoa's event requires to cover a greater extent area of around 15km^2. To reach the desired terrain extension more computational time is spent, which is why we consent lower spatial resolution. Mocoa's DEM has a cell size of 5m, and its coordinate reference system is MAGNA SIRGAS EPSG 3115. Based on the topographic analysis made by Pontificia Universidad Javeriana (2017), the available DEM has errors due to sumps and they detected some sectors with terrain elevation inconsistencies.

The initiation zones were obtained by visual examination through digital orthophotos, taken by an aerial survey. Different shapes and locations are tested with an iterative simulation process, but one place to start is upstream where there are steep slopes and scars have been observed. In Rebaixader, the initial area is placed in the scarp, and we restrict the domain to the areas with slopes greater than 30º. The preliminary simulations involved an unstable thickness range from 10cm to 60 cm which one switch until the expected initial volume is achieved. Considering that a small volume of initial mass can incorporate ten times or more of its volume as eroded material (Medina, et al., 2008). An analogous process is used for the Mocoa's initial area which is placed in the

steepest area. To reproduce the observed deposit in Mocoa, we have distinguished two initial areas, one in Taruca Creek and the other in Taruquita Creek.

The spatial domain is established in a Boolean data type file that can only take the values true or false. The true pixels represent the polygon where the passing flow is expected, including the initiation, propagation, and accumulation zones. The domain should be wide enough to avoid restricting the flow during a simulation. However, a small domain helps to reduce the computational time.

3.1.2 Calibration and validation model with historical events

Calibration is a trial-and-error process to set the right rheology parameters. The most efficient starting point is to know the input parameters through controlled laboratory tests. However, there are no available standard experiments to measure complex properties such as those of debris flows traveling at extremely rapid velocities (Pirulli, 2010). For this reason, the rheological parameters are constrained by systematic adjustment of a back-analysis. Measurements recorded and visual inspections are taken as the most important reference for the calibration. The representation of flow type (such as landslides, mudflows, debris floods, or debris flows) requires a flow resistance law suitable to describe the propagation and the stopping of the flow. In the case of debris flows, it is suggested a flow resistance law that is capable of describing frictional effects because of the coarse granulometry. Visco-plastic rheological laws like Bingham or Herschel-Bulkley are suitable for mud flows or fine-sediment debris flows (Papa, et al., 2018). Because the study episodes reported coarse granulometry, it is expected better results by employing the friction collisional Voellmy model (Medina, et al., 2008).

The method to calibrate the numerical simulation was the back-analysis whose purpose is to find the model parameters which can reproduce the reference results of the historical event (Heiser, et al., 2017). In other words, this method allows to calibrate the model, provided that the outcomes are close enough to the known results. Additionally, it is possible to simulate outcome variables

that were not measured during the real event. The researcher must identify not only the reference results but also need to define the evaluation concept to validate those results.

In a first approach, the flow resistance laws implemented into FLATModel are Bingham and Voellmy without entrainment with the Rebaixader initial conditions. Both models conserve the initial volume during the entire simulation, which neglects the effect of basal incorporation material. Bingham rheology requires defining the Bingham viscosity (μ_m) and the threshold basal shear stress (τ_0). The τ_0 can be determinate with the equilibrium equation for Bingham flows. In previous studies the typical values for τ_0/ρ range between 0.1-0.5 m^2/s^2 reaching even $1m^2/s^2$ for flow more turbulent (Medina, et al., 2008). For Bingham viscosity, the researchers suggest the μ_m concerning density (μ_m/ρ) around 0.05 m^2/s (Medina, et al., 2008). In our case, the best fit for Bingham rheology is setting with τ_0/ρ = 0.33 m^2/s^2 and μ_m/ρ = 0.05 m^2/s with a flow density of 2000 kg/m^3. Otherwise, the main input of the fluid model of Voellmy without entrainment is the Chezy coefficient (Cz) and the dry friction coefficient (μ). Based on sensitivity analysis, the term related to turbulent friction, Cz has predominantly impacted the velocity outcomes, meanwhile, the influence of the runout is given by $\mu = tan\varphi$. The best fit from the Rebaixader back-analysis encloses the possible range μ-values between 0.1 and 0.11 while Cz-values are ranging from 9.8 to 10 $m^{1/2}/s$.

In terms of basal erosion, the flow resistance law of Voellmy with entrainment is configured. The simulation of entrainment entails determining the bulk friction angle of the bed material (φ_{ent}), as well as the rheological parameters for Voellmy mentioned before Cz and μ. The selection of φ_{ent} is led by the bed material, but this parameter influences the final volume. In the case of Mocoa, the best configuration of the Voellmy fluid model is μ=0.07 due to the flat area in the fan, and Cz=10.3 $m^{1/2}/s$. The flow in Mocoa travels through an erodible bed of fractured Monzogranite, thus the internal friction angle of the bed material is about 30° or less. In the second case, Rebaixader involves many boulders along the erodible debs that interact with the bed material mobilized. Figure 9 presents two frames extracted from the event recorded, where it is reflected big boulders that suggest the entrainment of the wet bed typically of debris-flow paths. This demonstrates that φ_{ent} should result in a typical value for mixtures of gravel sands with few fines around 35°.

Figure 9. Scene acquired at different times in the Rebaixader's channel by the video camera. a) The flow at time 12:09:13. b) The flow three seconds after.

The model for Mocoa is validated against the previous studies and historical data. Considering the lack of known data for Mocoa's event, we develop a quantitative evaluation between the affected area and the simulated flow path. In this case, the error approach is described by adjusting the overlapping path areas. Also, it should be noted that only Voellmy with entrainment is regarded as the flow resistance law for numerical modeling. On the other hand, Rebaixader with the monitoring system enables us to assess more specific variables such as flow depth or flow velocity. The recorded data by the instrumentation and the information post-processing displayed in the histogram (see Figure 8) are used to validate the model against the flow depth in the debris flow front. The maximum flow depth measured by the radar is known and it is compared with the outcomes calibrated with Bingham, Voellmy without entrainment, and Voellmy with entrainment. The validation for each flow resistance law is achieved when the set rheological parameters are a proper choice for the best fit compared to the monitored data and the estimated volume.

3.2 Analytical methodology of boulders transport applied to Rebaixader

3.2.1 Single Rigid Block Model on an Inclined Plane

The boulders in the torrent are assumed to be represented by a frictional rigid block resisting on a plane with the respective terrain slope (θ). There are several numerical approaches to model the movement and interaction between individual blocks as the Discontinuous Deformation Analysis (DDA) based on dynamic equilibrium (MacLaughlin, et al., 2001). Considering the DDA models the kinematics of motion of individual blocks, this allows us to verify the numerical solution by analytical analysis (MacLaughlin, et al., 2001). Figure 10 shows a free-body diagram on an *x-y* plane, where the axes are parallel and orthogonal to the inclined plane. The forces W, F_r, and N are the weight of the block, the shear, and the normal force. The parameters φ and θ are the terrain slope and the internal friction angle. The dynamic equilibrium is defined as the sum of all the forces acting on the block in the *x* and *y* directions without external forces. The analytical solution for the block that rests under gravity acceleration (g) on an inclined plane θ is formulated with the resistance force in equation 5. Developing equation 5 where the coefficient of friction (μ) depends on the internal friction angle (φ=35°) and the weight is expressed as the multiplication of the density of the solids, the volume, and the gravity.

$$F_r = \mu N = \mu W \cos(\theta) \tag{5}$$

$$F_r = \tan(\varphi)\, \rho_{solid} V g \cos(\theta) \tag{6}$$

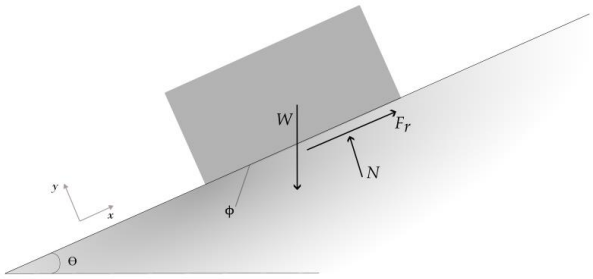

Figure 10. Rigid frictional block on an inclined plane.

3.2.2 Impact by Hydrodynamic Force

Debris flows are constituted by a mixture of wide-range size sediment. The influence of grain sizes is an essential factor in hydraulic properties. The grain-size distribution modifies the response of flow properties in terms of frictional shear resistance and pore-fluid pressure (Wang, et al., 2018). Fine grains content governs the rheology, while the coarse grains are responsible for macroscopic appearances such as the suspension of boulders on the flow surface, and the configurations of the surge front (Yong, L., et al., 2013). To estimate the impact force of debris flows, we used the models proposed for structural mitigation that are divided into hydraulic and solid collision. The hydraulic model (F_i) is classified as hydro-static and hydro-dynamic as described in equation 7. The analytical analysis is focused on the contribution of the first component of equation 7 that corresponds to hydrodynamic impact force.

$$F_i = a\rho_{debris} v^2 h_0 w + 0.5 k g h_0^2 w \tag{7}$$

Where a is the pressure coefficient, ρ is the density of the debris flow in kg/m^3, and v is debris velocity at impact in m/s. The second term is the hydrostatic force which has the static impact coefficient k, and gravity g. Both terms have in common the variables of debris thickness h_0, and debris width w, in meters. However, this force can be understood as a force per unit area,

transforming the force equation into a minimum value of pressure (p_i) with a factor of ½ as shown in equation 8, or a maximum pressure, p_{max} (equation 9).

$$p_i \approx \frac{1}{2}\rho_{debris}v^2 \tag{8}$$

$$p_{max} \approx a\rho_{debris}v^2 \tag{9}$$

The empirical factor (a) depends on the flow type, where values about 2.0 are recommended for laminar flow and fine-grained, but for coarse-grained materials, the value must be higher than 4.0 (Hübl, et al., 2009). Rebaixader site has a high concentration of sediments with a wide granulometry, so 2.5 will be considered for the increase factor in equation 9 (p_{max}). According to the previous equation, the variation of the impact pressure as a function of mean velocity is plotted. Figure 11 shows the behavior of impact pressure p_i and p_{max} as a function of mean velocity with a constant terrain slope of 30°. The mean velocity of the plot is based on the outcomes from Voellmy with entrainment simulation along the flow trajectory. It is observed that the pressure has exponential behavior, considering the hydro-dynamics model with a factor of increase grows much faster.

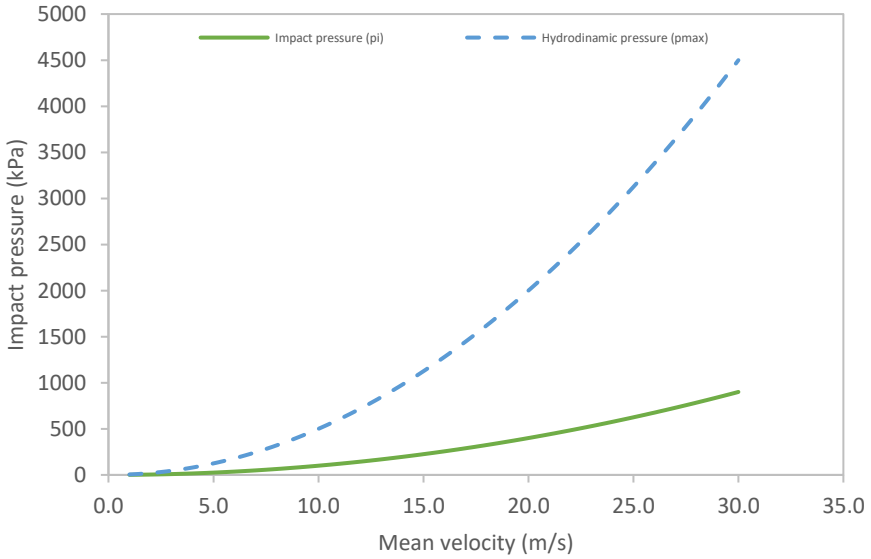

Figure 11. Impact pressure p_i and p_{max} behavior as a function of mean velocity.

4. Results and Discussion

4.1 Back-analysis of the 2017 Debris Flow in Mocoa

The back-calculation technique was applied to calibrate and validate the parameters of the Voellmy model with entrainment in FLATModel. Because the only reference information to perform the simulations is the shape of the inundated area, initially we focus on the propagation and deposition path. Several simulations were developed to carry out a sensitivity analysis of the rheological parameters. The back-analysis covers the flow behavior along the Taruca and Taruquita creek assuming an initial volume of 1163 m^3 and omitting the subsequent events. The neglect of the temporal dimension added difficulty to define a time of departure for each creek. This is because the numerical modeling starts the movement with the entire initial volume at time zero.

The open sources of the geographic information system of the Colombian Geological Service (SGC) have DEMs of different resolutions. The selection criteria are to consider the terrain elevations before the event and the more detailed DEMs available (spatial resolution of 2m and 5m). A preliminary evaluation was performed using the DEM with 2m resolution to find the configuration of the rheological parameters. The drawback is that the model takes more than a day to run one simulation and the calibration requires an iterative process of simulations. That is why we selected the DEM with a cell size of 5m which was used to perform the back-analysis of the 2017 Mocoa event. The sensitivity analysis of the three main rheological parameters of Voellmy with entrainment was developed comparing the simulated path with field observation and satellite images. The best-fit simulation was obtained by μ=0.07, Cz=10.3 m½/s and φ_{ent}=28.4°. Figure 12 and Figure 13 illustrate the maximum flow depth and maximum velocity respectively along the torrent where the inundation area is compared for a computational time of 1000s and 1300s. In the first perception, the simulated flow adjusts to the area registered in the field, but it seems to overflow the established polygon boundaries. Additionally, the computational time of 1000s is not enough for the flow to reach the fan, while increasing the time results in a longer path.

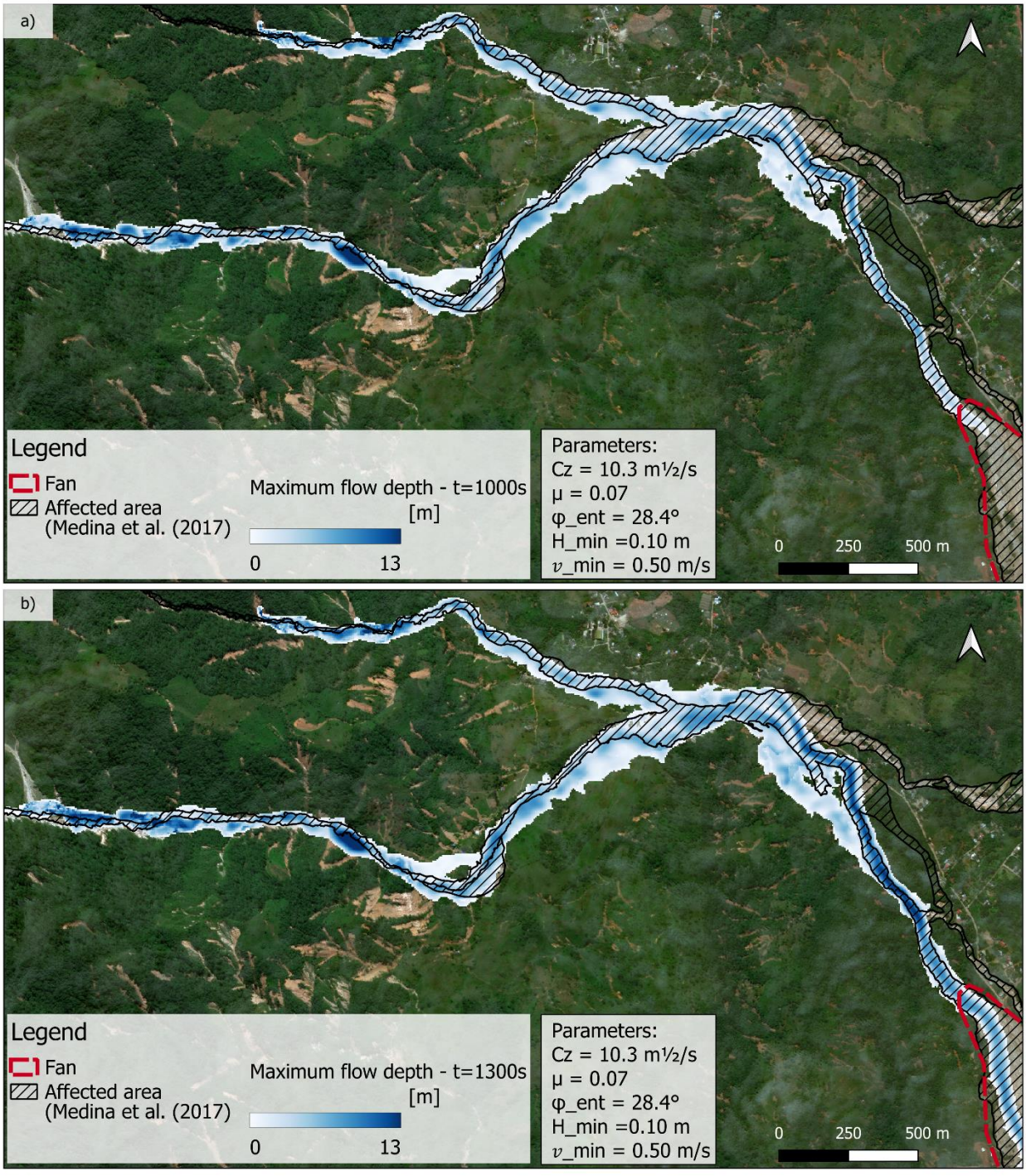

Figure 12. Maximum flow depth modeled for Voellmy with entrainment flow resistance law: a) Computational time t= 1000s, b) Computational time t=1300s.

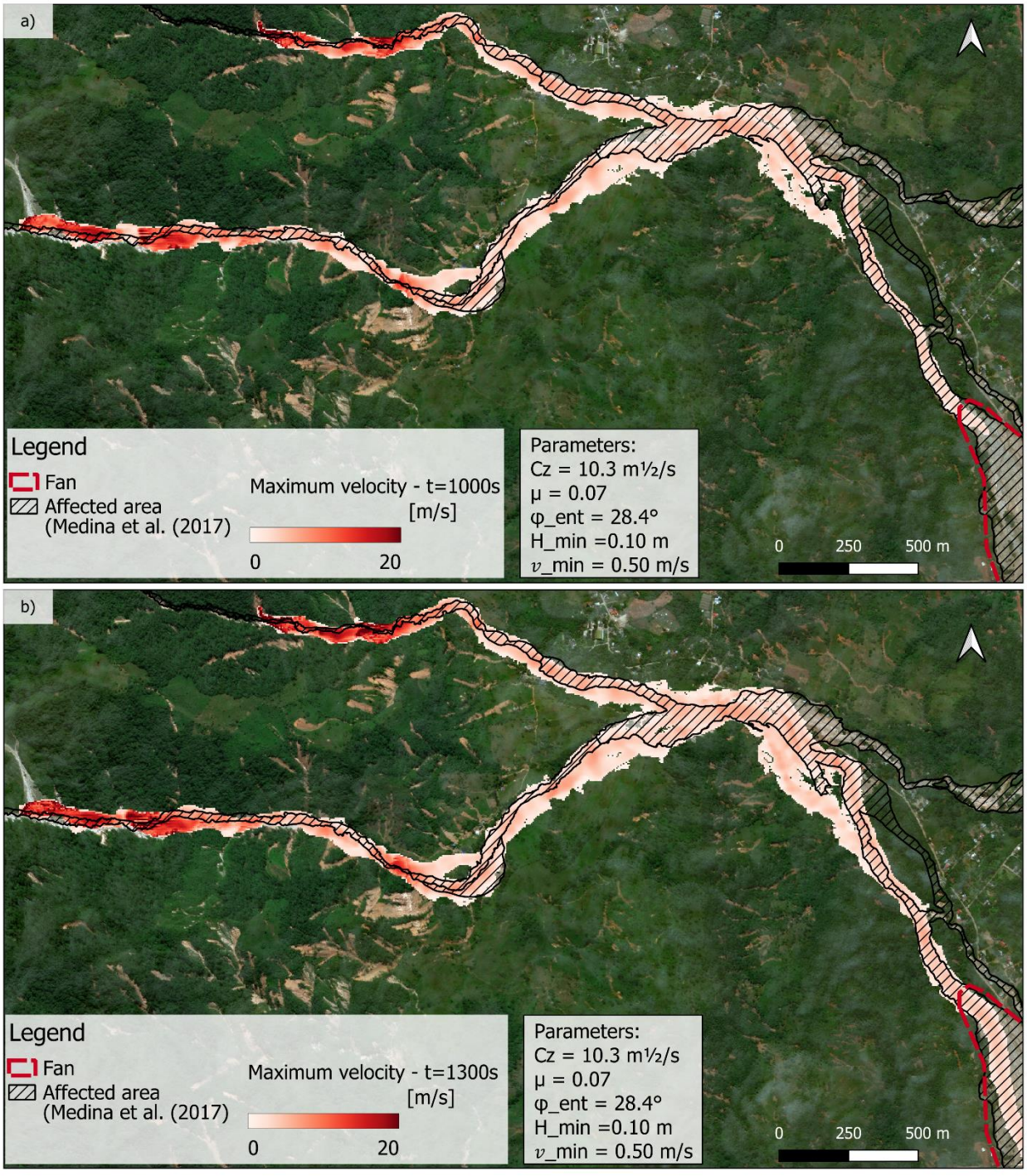

Figure 13. Maximum velocity modeled for Voellmy with entrainment flow resistance law: a) Computational time t= 1000s, b) Computational time t=1300s.

Remarkably, the shape of the resulting deposit does not match the reported deposit width since the simulated flow still has a narrow width and appears channelized. This behavior ignores what happened due to the flow running into the urban infrastructure and making its way between the streets. To represent the effect of urban infrastructure the model needs to be equipped with the arrangement of obstacles that restricted the flow such as buildings, trees, or light posts. FLAT-Model by the file of domain enables to set up of the path through which flow is allowed. This aspect was not considered but it is suitable for improving the outcomes in the fan regarding future reviews. The idea for future review would be to introduce all the elements of the fan that disturb the flow (for example the buildings as seen in Figure 14) to complement the domain file with pass restrict the rule to evaluate the urban infrastructure interaction. Now, the best scenario is achieved by running t=1300s as the flow can reach the fan and give time to build up sedimentary material. In addition, this simulation provides a good agreement between the simulated total volume of $2.8x10^6$ m^3 with $3x10^6$ m^3 reported by the SGC.

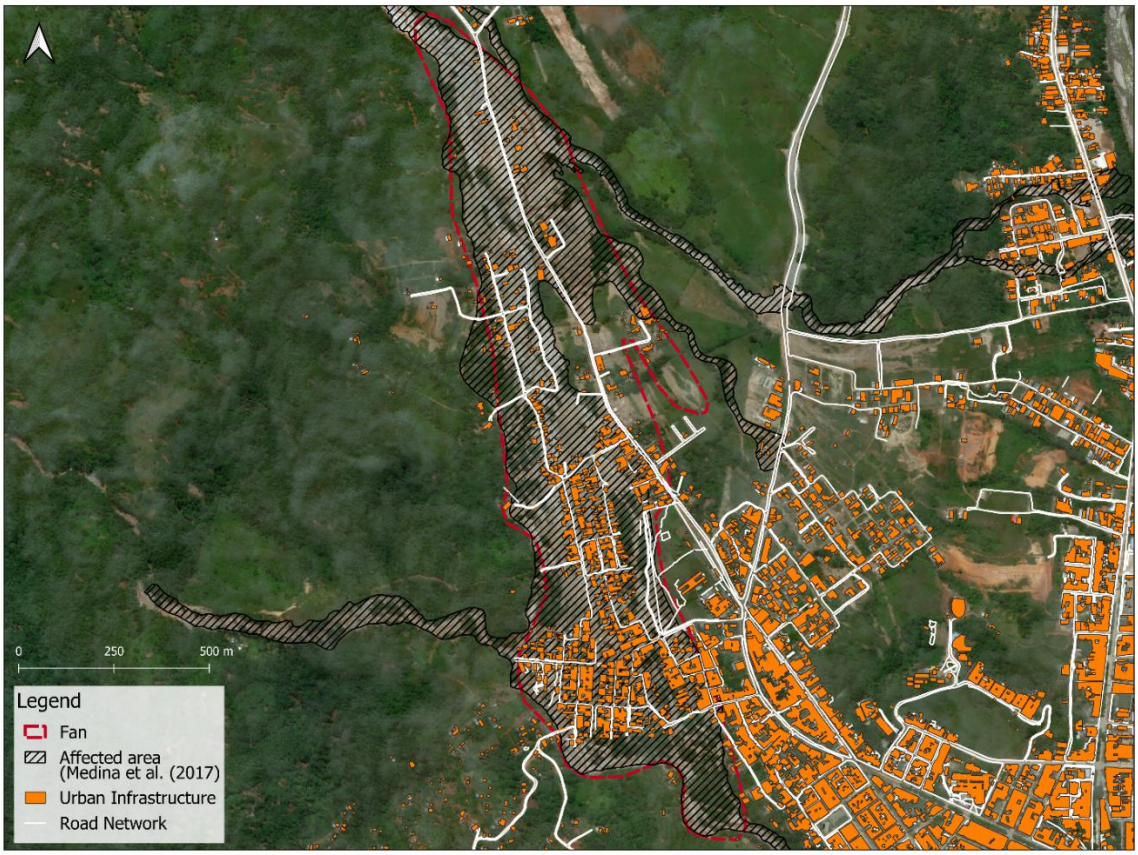

Figure 14. Urban infrastructure data in the Mocoa fan.

In the absence of monitoring devices along the basin, the validation of the numerical simulation outcomes was carried out by using the field reports after the event. Moreover, the optimal results are accompanied by a literature review and assessment of assumptions. Thus, it should be kept in mind that the DEM provided by SGC has inconsistent elevations reported in Pontificia Universidad Javeriana, 2017. They also concluded that despite the drawback, the available DEM is in better agreement with the observed drainage and satellite images (Pontificia Universidad Javeriana, 2017). The least consistent elevations are outlined in the fan and before the convergence point of the creeks (Pontificia Universidad Javeriana, 2017). The modified DEM was not published, and its changes were about ±1.5m according to their field observations. Consequently, we generated Figure 15 where is shown a mapping of the maximum flow depth ranging from 1m to 13m to enhance the path match.

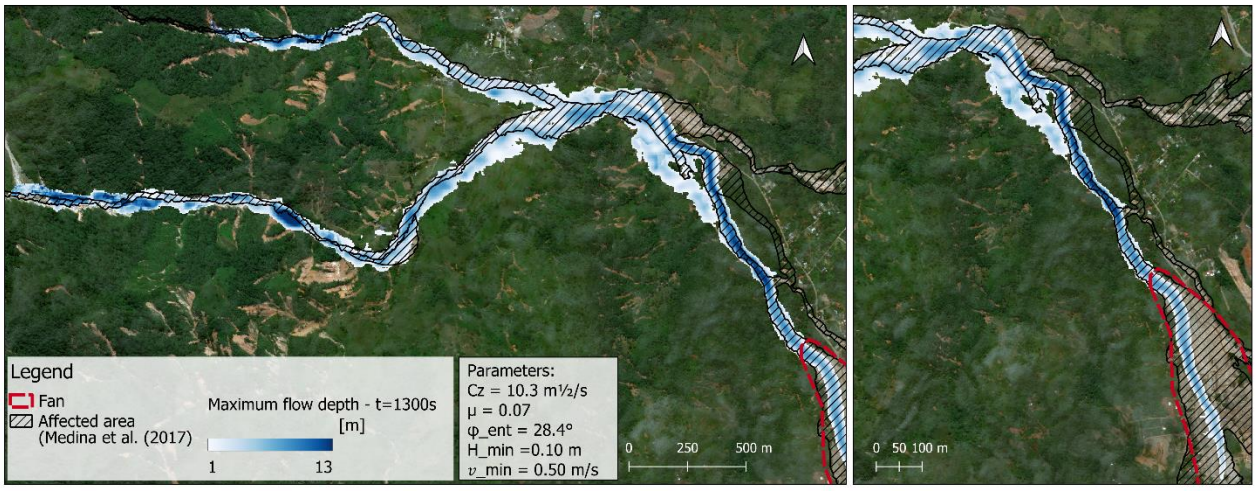

Figure 15. Maximum flow depth modeled for Voellmy with entrainment zoom in at the fan zone.

The magnitude of the debris flow event under study resulting in major damages to the population and infrastructure, not only because of the large volume mobilized but also because of the size of the blocks. The transported boulders were of such a size that explosives were needed to remove them (Pontificia Universidad Javeriana, 2017). For this reason, the design of protection measures in Mocoa involves 20m high dams, and some of them are along Taruca creeks and Sangoyaco River already operating (Pontificia Universidad Javeriana, 2017). Therefore, the implementation of entrainment in the simulation suggests a success because much of the transported material was due to erosion and not only from landslides.

4.2 Back-analysis of the 2020 Debris Flow in Rebaixader

Modeled results and monitored data were compared by types of outcomes. On one side the hydrographs measured by the radar sensor and the ones simulated by FLATModel at the position of this sensor were evaluated. On the other side, the observed erosion depths, which were obtained by the DEM of Difference (DoD) from the UAV surveys, were compared with the ones calculated by the entrainment modeled with FLATModel.

FLATModel simulated the event at Rebaixader with three flow resistances law. Many different simulation runs were executed to calibrate the corresponding parameters of each model until getting the parameters in Table 3. The most important location in the simulation domain was at the end of the channel, where the flow-depth sensor is installed. Therefore, at this point, the flow characteristics are known, and the volume estimation is 10000 m^3. Figure 16 illustrates the simulated maximum flow depth, and Figure 17 presents the maximum velocity, both for the three flow resistance laws. The maximum flow depth values can reach more than 3 m, while the range of the maximum velocity is more sensitive to the variation of the resistance law. The first approach was applying Voellmy fluid that gave a good fit of the flow characteristics with the parameter combinations of C_z=9.8 $m^{1/2}/s$ and $\mu=\tan\varphi$=0.11. The simulation improves by contemplating the effect of entrainment and therefore, the final best-fit values of the input properties are C_z=11.2 $m^{1/2}/s$, $\mu=\tan\varphi$=0.15, φ_{ent}=36.2°; and the minimum flow depth (H_min) and velocity (v_min) are established at 0.10 m and 0.50 m/s respectively. In contrast, the best-fit Bingham parameters were 0.66 kPa for the threshold basal shear stress (τ_0), μ_m=0.1 kPa s, and ρ=2000 kg/m^3. The simulations applying Bingham rheology do not give very reliable results because the behavior does not describe correctly the one observed. After adjusting the rheological parameters for each flow resistance law, the outcomes were compared (see Figure 16 and Figure 17). One of the reasons for this is attributed to the fact that the Voellmy expression of the basal shear stress requires determining a value of the terrain slope to start moving (Medina, et al., 2008). Besides, viscous Bingham parameters were calibrated, and laminar behavior was ruled out because the flow was turbulent. Nevertheless, the outcome from the calibration was not satisfactory, despite the optimization, so this restates that this rheology is inappropriate to reproduce the event.

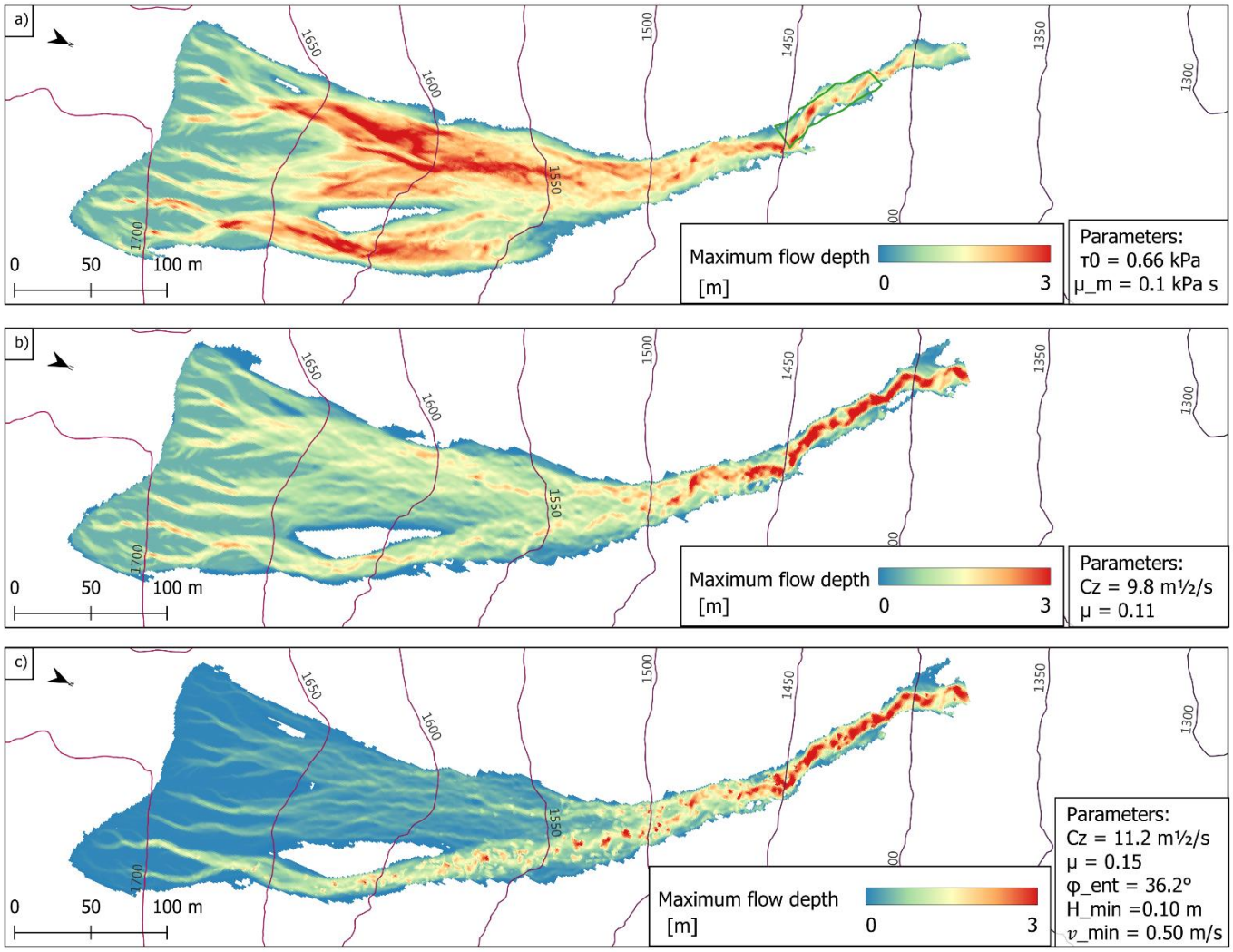

Figure 16. Maximum flow depth modeled for the three different flow resistance laws: a) Bingham, and b) Voellmy without entrainment. c) Voellmy with entrainment.

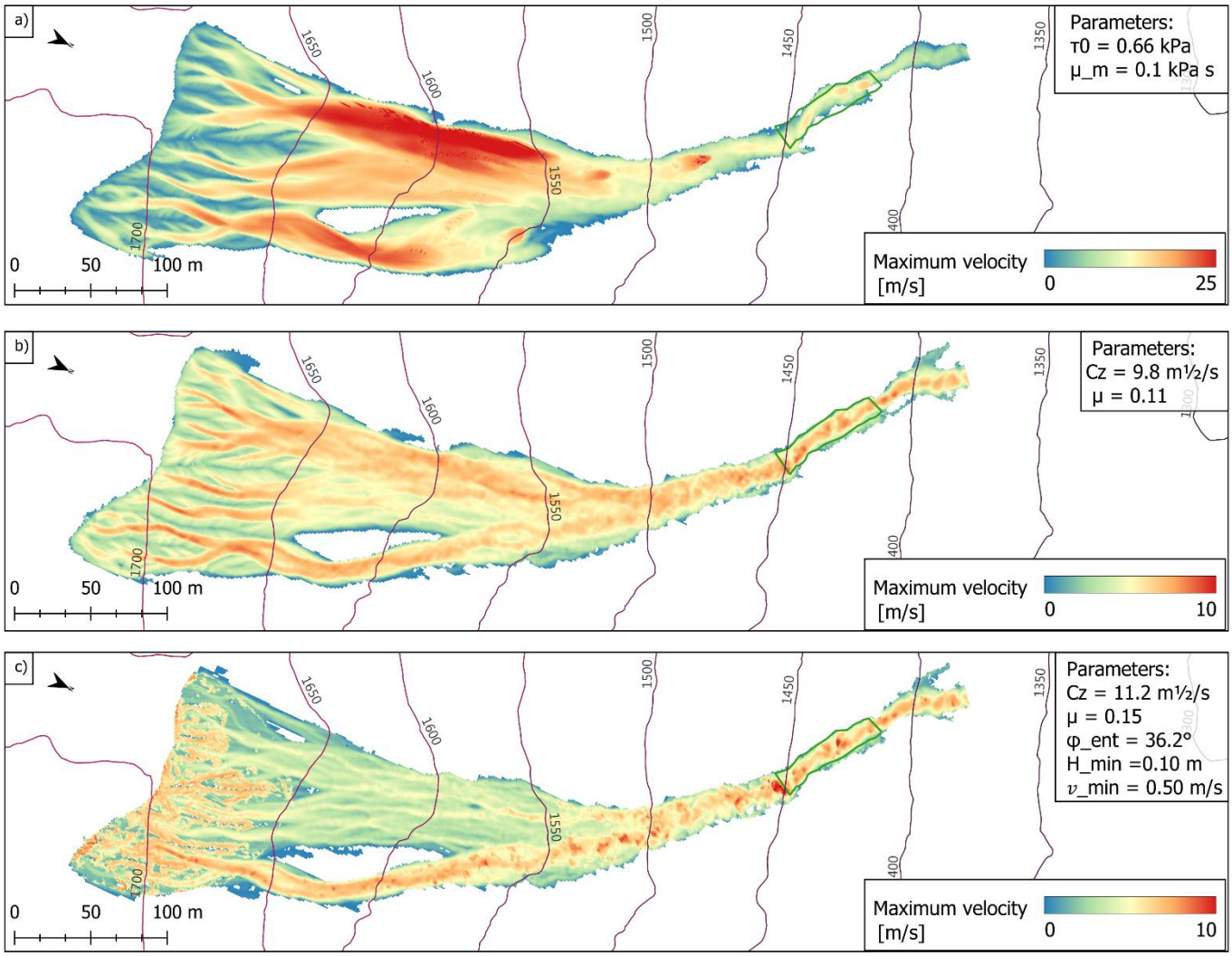

Figure 17. Maximum velocity modeled changing the flow resistance law: a) Bingham, b) Voellmy without entrainment. c) Voellmy with entrainment.

Table 3. Summary of the calibrated parameters of the modeling.

PARAMETERS	μ_m	τ_0	**Cz**	**μ = tanφ**	**φ_ent**	**H_min**	**v_min**
	[kPa s]	[kPa]	[m½/s]	[-]	[°]	[m]	[m/s]
MODELLED BINGHAM	0.1	0.66					
VOELLMY WITHOUT ENTRAINMENT			9.8	0.11			
VOELLMY WITH ENTRAINMENT			11.2	0.15	36.2	0.1	0.5

The hydrograph in Figure 18 shows a comparison between the modeled results and the monitored with the radar at the channel. Maximum flow depth reaches a few seconds after the front crosses the radar, but the maximum velocity is obtained just in the front. In Figure 18, the peak measured was 1.6 m which fits better with Voellmy entrainment modeling regarding all the measured behavior. Additionally, Table 4 allows us to compare the outcomes because it contains the maximum flow depth, maximum velocity, and the estimated volume for the simulations and the monitored. The best-fit model considers both the maximum flow depth and the mean velocity at the highest flow front at the location of the radar sensor. In the case of Voellmy with entrainment, a peak of 1.67 m and velocity of 5.28 m/s were shown, while the results without the effect of basal erosion are 2.85 m and 4.24 m/s. In contrast, the Bingham model returns a result of 1.35 m for maximum depth and a velocity of 8.13 m/s. For Voellmy with entrainment, the percentage of error regarding the maximum flow depth measured is 7.1% which is much less than an error of 82.4% with the plain model. However, the percentage of error with Bingham rheology is 13.5% for the maximum flow depth, but the mean velocity is twice the field estimated.

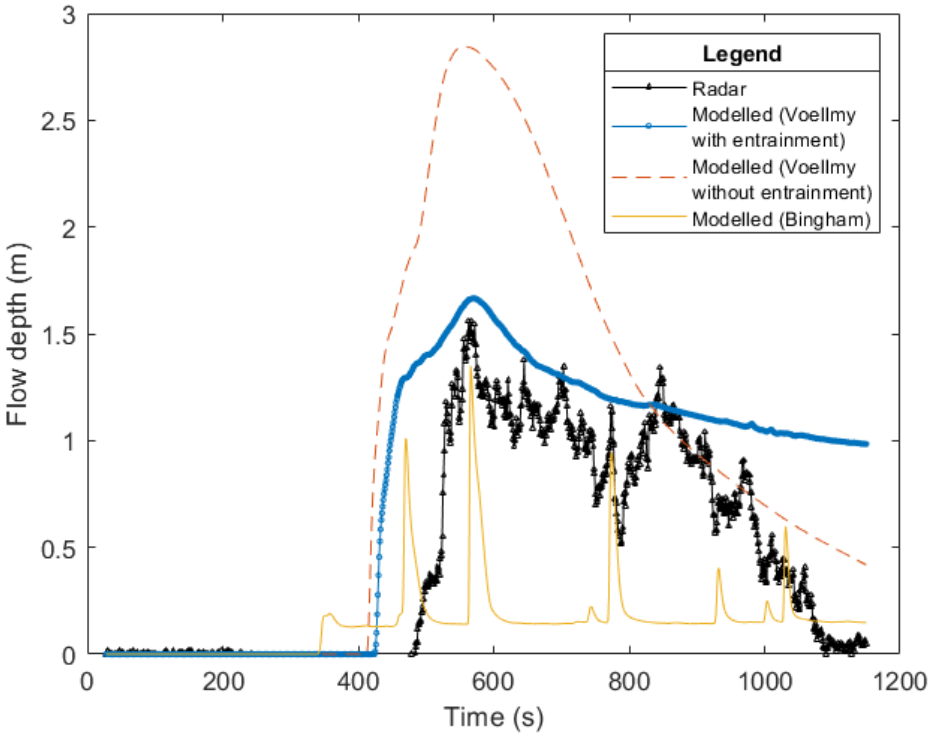

Figure 18. Comparison of monitored and modeled hydrographs for the July 2020 debris flow at the location of the radar sensor.

Table 4. Comparison of the modeled outcomes and monitoring data at the place of the radar.

TYPE OF OUTCOMES	**MAXIMUM FLOW DEPTH**	**MAXIMUM VELOCITY**	**VOLUME**
	[m]	**[m/s]**	**[m³]**
Monitored	1.6	4.10	9228-10810
Modeled Voellmy with entrainment	1.67	5.28	10697
Modeled Voellmy without entrainment	2.85	4.24	7897
Modeled Bingham	1.35	8.13	7897

The debris flow can travel through a non-erodible or erodible torrent. Where the non-erodible surfaces refer to the bottom with bedrock. One challenge for the numerical models is the entrainment of materials from erodible beds. FLATModel can simulate entrainment as mentioned in previous chapters, but it does not distinguish the zones with the bedrock. In Rebaixader, the scarp and the funnel have loose material erodible, while in the channel there are some areas with bed rocks as is observed in Figure 19. Besides, there is a complex process of the mass exchange between the debris flow layer and the erodible bed that occurs along steep and irregular terrain which requires spatial discretization (Martínez-Aranda, et al., 2022). In Figure 19, the DoD shows some accumulation of eroded material behind the big blocks that FLATModel represents as erosion. To reproduce a more detailed terrain, a significant increase in computational processing time arises due to the additional equations needed to give more terrain features.

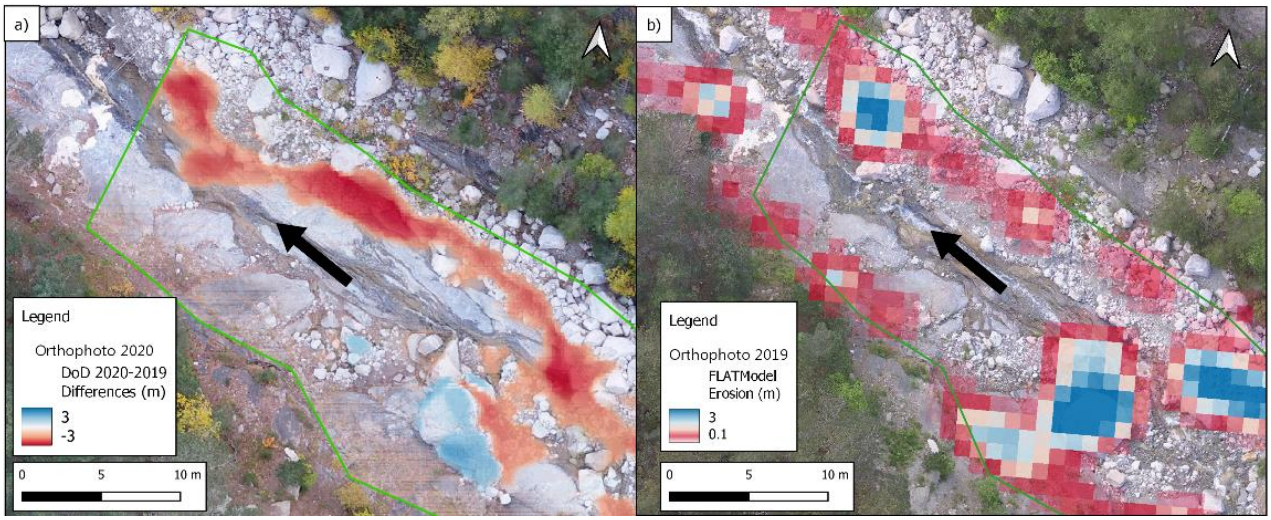

Figure 19. Rebaixader's erosion depth. a) DEM of Differences based on data of UAV. b) Erosion simulated by FLATModel with Voellmy with entrainment.

4.3 Analytical Application of Impact and Transport of Boulders

4.3.1 General Aspects

The goal of this section is to carry out an analytical analysis of the effect of entrainment taking stock of big blocks in Rebaixader. Debris flows transport a large amount of sediment with a wide range of sizes, which are gained by entraining material as the flow descends steep slopes and channels (Iverson, et al., 2011). Their destructive power has promoted the development of structural mitigation measures. To define the design, it is required to determine the impact force. The impact processes can be described in three stages. First, a powerful impact occurs due to the debris flow head, then the flow body impacts continuously and steadily, and at the end appeared the tail of debris flows that slips with less velocity (Cui, et al., 2015). In our case, the Rebaixader site does not have mitigation measures to prevent the process or infrastructures to limit the damage. Under these circumstances, big boulders move down through the torrent to the fan, and this is identified for the event of 2020 as shown in Figure 20.

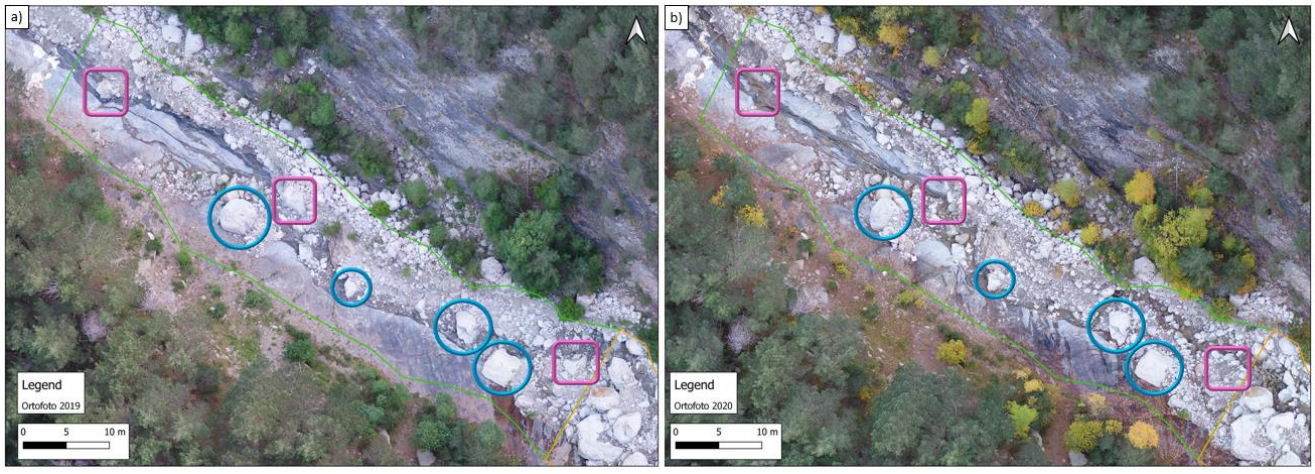

Figure 20. Identification of mobilized (pink rectangle) and stable (blue circle) blocks. a) Channel reach orthophoto in 2019 before the event. b) Channel reach orthophoto in 2020 after the debris flow.

4.3.2 Application to Rebaixader Site

The presence of big blocks in Rebaixader incites the analysis of the critical boulder size that the 2020 event mobilized. The critical radius (r_c) equation (equation 10) is defined by applying equations 6 and 8 in units of force, assuming spherical boulders. Note that is used equation 8 as the minimum pressure, because there is a stop effect with the passing of the flow, and we are interested in finding the minimum impact force to translate the blocks. In the beginning, there is a direct impact of the flow to the boulder, but after some time the flow will go around the boulder and some material will be deposited behind the boulder that is contributing to stopping it. We assume the first impact is high enough to impact the block but not move it. While the total energy of the impact is used to push the block, the remaining energy is not able to translate the boulder, only to move a bit. The critical radius represents the threshold to start the movement. Thus, if the radius values in the zone of analysis are above critical one, those boulders remain at rest, otherwise, the flow gains new material. Figure 21 plots the variation of the impact pressure for a terrain slope of 30º depending on the critical radius. To compare different terrain slopes, Figure 22 presents different series of slopes to describe the increase of the critical radius when the mean velocity rises.

$$r_c \approx \frac{0.375\rho_{debris}v^2}{\tan(\varphi)\, g\rho_{solid}\cos(\theta)} \tag{10}$$

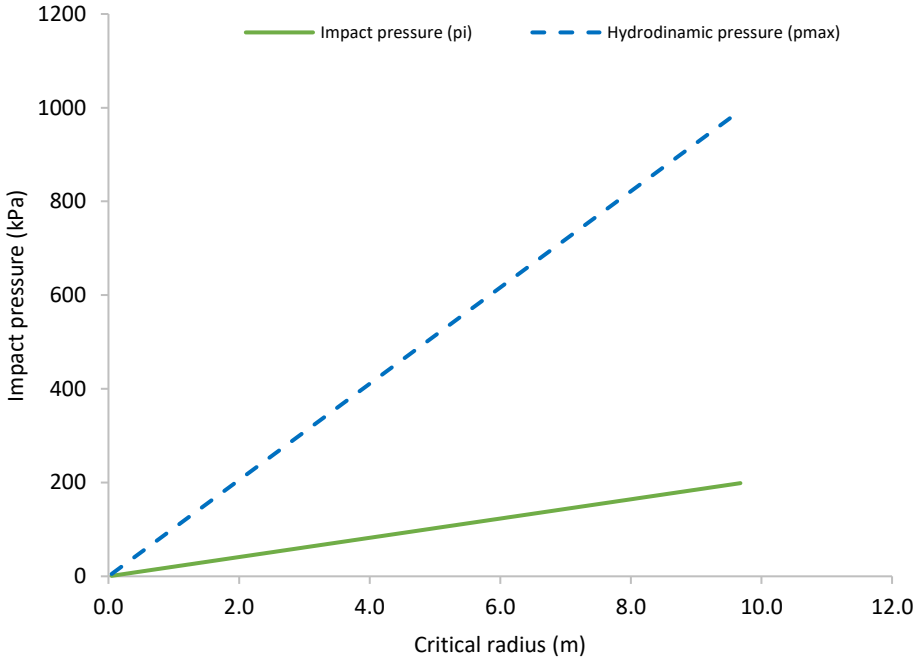

Figure 21. Critical radius as a function of impact pressure with a constant terrain slope of 30°.

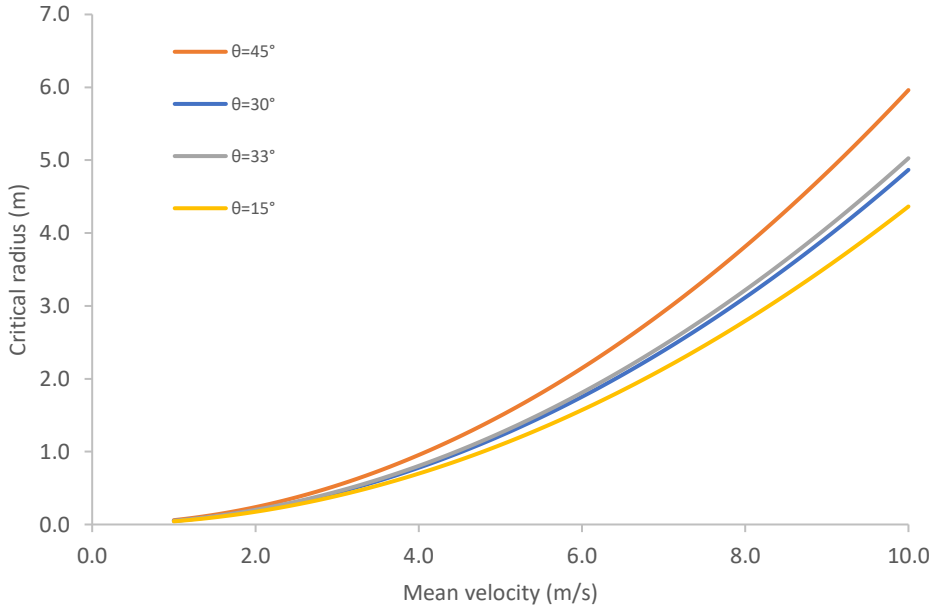

Figure 22. Critical radius as a function of mean velocity for different slope terrain angles.

Based on the available Digital Elevation Model (DEM) of 2019 with a cell size of 1x1m, we extracted a longitudinal profile of terrain slope angles. Besides it is considered to take a standard value of internal friction angle for mixtures of gravel-sand with few fines of 35° and debris density of 2000 kg/m3. Also reviewing the study of the granulometric properties, we found the density of the solids in the Rebaixader basin is 2590 kg/ m3. The incorporation of the above information in equation 10 allows us to generate a distribution of critical radius. Once the distribution of the critical radius is obtained, Figure 23 is developed where it is observed the correlation between the critical radius and the mean velocity using the minimum and maximum impact pressure formulation.

Additionally, it can be observed in Figure 20 that the missing blocks when the orthophoto in 2019 and 2020 were compared. Through the simulation with Voellmy with entrainment it is possible to know the velocity when the maximum flow depth impacts each identified block at the channel. Also, the radius of each boulder was set up with the visual estimation of the orthophoto. The boulders are included in Figure 23 distinguishing two types of marks (stable and mobilized) and considering an uncertainty of 20% because of the upstream block surface covered by sediment. All the mobilized blocks are above the curve of velocity associated with minimum impact pressure (p_i). One of them required a higher velocity as well as a hydrodynamic impact. Regarding the stable ones, it is observed two blocks are above the curve related to minimum impact pressure. This means the debris flow would have needed more velocity at the moment of impacting these blocks.

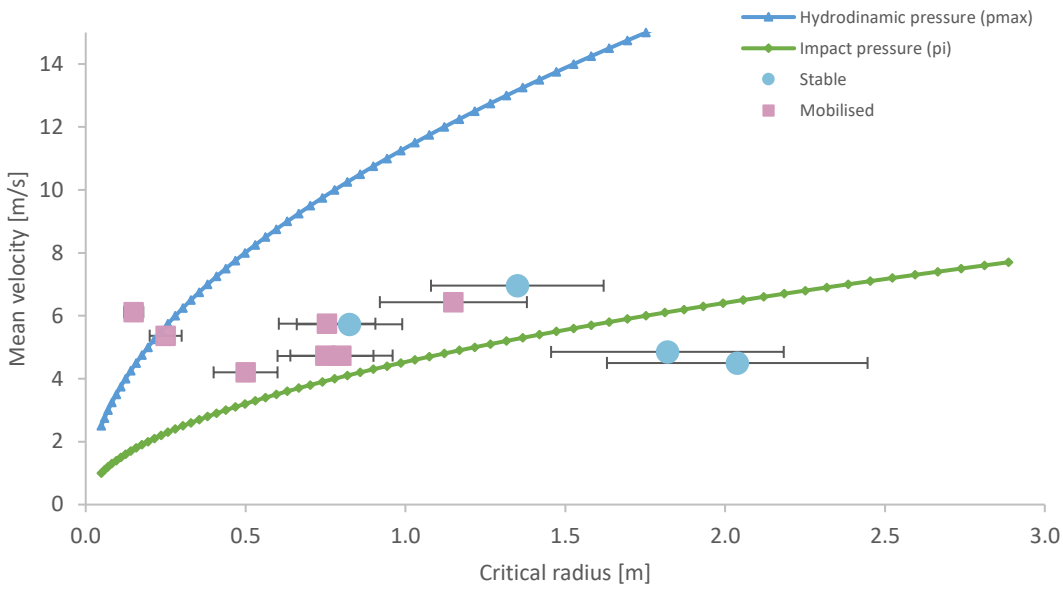

Figure 23. The critical radius as a function of mean velocity for a terrain slope of 30° identifies the critical radius for stable and mobilized blocks during the event with an associated error of 20%.

A practical application of all previous results may be indicating the spatial distribution of the critical radius as shown in Figure 24. The investigated case study can be mapped by critical radio (Figure 24) to predict the zone where eroded material is added more easily. The intensely red areas in Figure 24 are mostly contained in the upper part of the scarp and in the channel where the critical radius is an order of magnitude above the meter. This agrees with the fact that the terrain slope in the scarp is the highest and the volume grows rapidly. In this investigation, we focus on the erosion of the channel because of the availability of information. Thus, it is possible to post-process the erosion depth modeled after the identification of the big boulders and the bedrock.

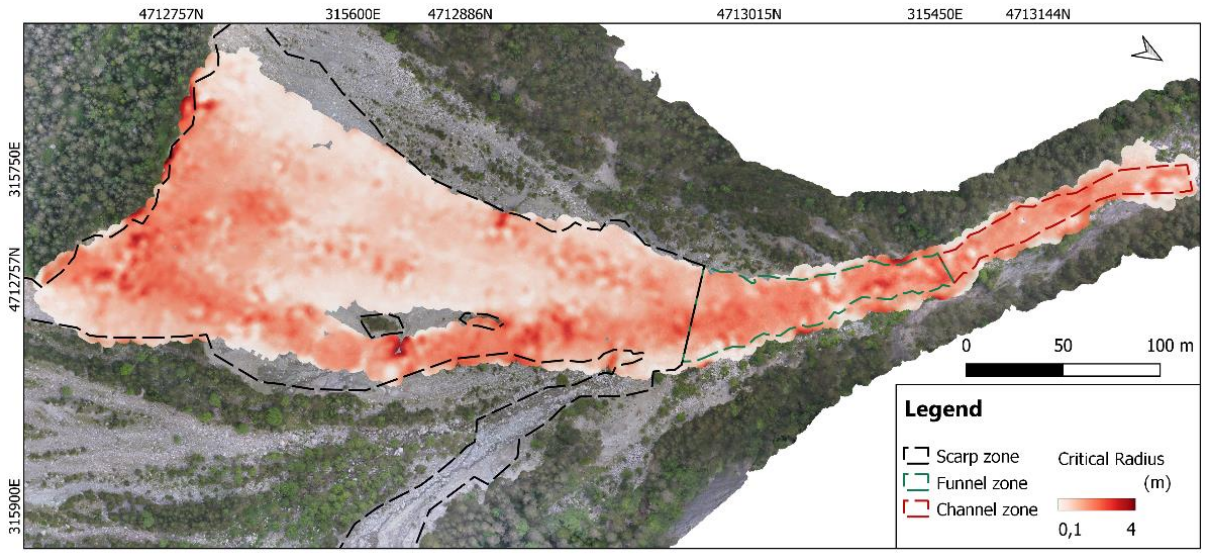

Figure 24. Spatial distribution of critical radius along the Rebaixader basin.

Determination of the entrainment is a key step in the prediction of debris flow magnitude and behavior with the difficulties of obtaining data on entrainment depth, and then correlating these data with the flow resistance law parameters (Jakob & Hungr, 2005). One challenge of the simulation of debris flow is the prediction of the volume without the entrainment of sediment. The implementation of entrainment in a runout model can improve the quality of the prediction of flow patterns due to better accuracy of the flow depth and discharge of the flow (Frank, et al., 2015). Generally, the entrainment is caused by erosion and bed destabilization as a result of drag forces acting at the base of the flow (Jakob & Hungr, 2005). Another important fact is the dependency of the entrainment on the local terrain slope. In consequence, the threshold of the terrain slope to start the erosion may change from one event to another, or between individual surges (Jakob & Hungr, 2005). The mapping of critical radio is a way to characterize vulnerability from debris-flow impact based on the destructive ability of the flow. This method is convenient and repeatable to estimate the most threatened areas within a hazardous region from debris flow. Therefore, the assessment provides useful information to support landslide risk management. More often the quantitative debris flow risk assessments form the basis of decision-making on the engineered mitigation measures (Jakob, et al., 2012).

5. Conclusions

Entrainment during debris-flow events is an important aspect of hazard assessment and the calibration of rheological and entrainment parameters is a complex task. The results of this study confirm the importance of debris-flow modeling to understand and describe the flow dynamics using back-analysis. The numerical code FLATModel was applied to two real cases in Rebaixader and Mocoa. The reconstruction of the events involved available data from previous studies, field measurements, and monitoring data.

The historical disaster event of 2017 in the Mocoa basin occurred because of four days of high-intensity rainstorms during the rainy season (La Niña event). Other factors contributed to the scale of the damage in terms of property loss and ecological environment. One of the major factors is hillslope instability added to the erosion process along the torrent. The present work has only been performed in the Taruca and Taruquita Creeks focusing on the mass movements which correspond to debris flows. Several simulations were required to adjust the Voellmy fluid model parameters with entrainment and to obtain the best fit. The final selection of the rheological parameter was μ=0.07, *Cz*=10.3 m½/s and φ_{ent}=28.4°. The Digital Elevation Model (DEM) of the extent before the event was necessary for the back analysis with a reasonable spatial resolution of 5m, although some uncertainties were reported. The temporal sequence of different mass releases represents a limitation to simulate what happened. Another drawback is related to the absence of exact measurements of the flow depth or flow velocity due to the lack of instrumentation. Despite these uncertainties, the simulated final volume setting Voellmy with entrainment coincides rather well with data reported by the SGC and previous studies based on field observations.

Regarding the Rabaixader case, the implementation of different flow resistance laws was applied to FLATModel. The Rebaixader DEM has better resolution than Mocoa DEM due to monitoring with the geomatic technique of digital photography from UAV. The simulation results indicated the best fit is achieved by including the effect of basal erosion along the flow trajectory employing Voellmy with entrainment parameters (C_z=11.2 $m^{1/2}$/s, μ=tanφ=0.15, φ_{ent}=36.2°). Thus, a real benefit of monitoring systems is seen in the sense of permitting the comparison

between measured and modeled data. Another advantage is the possibility to assess the DoD technique which confirms cell-by-cell the change in elevation between pre- and post-event topography. The results of DoD are contrasted with the final topography obtained from the simulation. This admits to the conclusion that debris flows are formed by the progressive incorporation of sediment material from the erodible bed during the entrainment process.

The analysis of the impact and transport of boulders established a baseline to understand the sensitivity analysis of the rheological parameter φ_{ent}. The video recording of the 2020 event let us see many big boulders in the flow front and the orthophotos of 2019 and 2020 confirm that there are missing blocks along the torrent. This raises the question of the maximum boulder size that can be transported which is not uniform throughout the basin. The impact and transport capacity is mainly influenced by the terrain slope and the flow velocity. This study describes the critical radius to illustrate the susceptible areas where the flow develops a more destructive capacity and can mobilize a larger boulder size.

Regarding future research lines, it is proposed the study on the stabilization of hillslopes and controlled drainage of debris flows. Part of the following works should focus on the entrainment of bed material as characteristic feature behavior of debris flows. Considering debris flows gain much of their mass and destructive power by entraining material, the evaluation of the critical radius is promoted. Because the debris flows mitigation measures are still in innovation processes, a method is needed to determine the most suitable location along the torrent to minimize damage. Moreover, the prediction of the debris flow path must be evaluated by the incorporation of an accurate representation of the topography. For this reason, future studies will considerably improve the modeled results by exploring the benefit of the domain file of FLATModel with which it is possible to include the urban infrastructure data.

References

Arattano, M., Franzi, L. & Marchi, L., 2006. Influence of rheology on debris-flow simulation. *Natural Hazards and Earth System Sciences,* Volume 6(4), pp. 519-528.

Baggio, T., Mergili, M. & D'Agostino, V., 2021. Advances in the simulation of debris flow erosion: The case study of the Rio Gere (Italy) event of the 4th August 2017. *Geomorphology,* Volume 381, p. 107664.

Cesca, M. & D'Agostino, V., 2008. Comparison between FLO-2D and RAMMS in debris-flow modelling: a case study in the Dolomites. *WIT Transactions on Engineering Sciences,* Volume 60, pp. 197-206.

Cui, P., Zeng, C. & Lei, Y., 2015. Experimental analysis on the impact force of viscous debris flow. *Earth Surface Processes and Landforms,* Volume 40(12), p. 1644–1655.

Frank, F., McArdell, B. W., Huggel, C. & Vieli, A., 2015. The importance of entrainment and bulking on debris flow runout modeling: examples from the Swiss Alps. *Natural Hazards and Earth System Sciences,* Volume 15(11), pp. 2569-2583.

Frank, F., McArdell, B. W., Oggier, N. & Baer, P., 2017. Debris-flow modeling at Meretschibach and Bondasca catchments, Switzerland: sensitivity testing of field-data-based entrainment model. *Natural hazards and earth system sciences,* Volume 17(5), pp. 801-815.

Fuchs, S., Heiss, K. & Hübl, J., 2007. Towards an empirical vulnerability function for use in debris flow risk assessment. *Natural Hazards and Earth System Sciences,* Volume 7(5), pp. 495-506.

García-Delgado, H., Machuca, S. & Medina, E., 2019. Dynamic and geomorphic characterizations of the Mocoa debris flow (March 31, 2017, Putumayo Department, southern Colombia). *Landslides,* Volume 16(3), pp. 597-609.

García-Ruiz, J. M., Beguería, S., Lorente, A. & Martí Bono, C. E., 2002. Comparing debris flow relationships in the Alps and in the Pyrenees. *CSIC - Instituto Pirenaico de Ecología.*

George, D. L. & Iverson, R. M., 2014. *A depth-averaged debris-flow model that includes the effects of evolving dilatancy. II. Numerical predictions and experimental tests.* s.l., s.n., p. 470(2170).

Gómez, J. & Montes, N. E., 2020. *Mapa Geológico de Colombia en Relieve 2020. Escala 1:1 000 000,* s.l.: Servicio Geológico Colombiano.

Heiser, M., Scheidl, C. & Kaitna, R., 2017. Evaluation concepts to compare observed and simulated deposition areas of mass movements. *Computational Geosciences,* Volume 21, pp. 335-34.

Hübl, J.; Suda, J.; Proske, D.; Kaitna, R.; Scheidl, C., 2009. Debris flow impact estimation. *Proceedings of the 11th international symposium on water management and hydraulic engineering,* Volume 1, pp. 1-5.

Hürlimann, M., Abancó, C., Moya, J. & Vilajosana, I., 2014. Results and experiences gathered at the Rebaixader debris-flow monitoring site, Central Pyrenees, Spain. *Landslides,* Volume 11(6), pp. 939-953.

Hürlimann, M., Rickenmann, D., Medina, V. & Bateman, A., 2008. Evaluation of approaches to calculate debris-flow parameters for hazard assessment. *Engineering Geology,* Volume 102(3-4), pp. 152-163.

Iverson, R. M., 1997. The physics of debris flows. *Reviews of geophysics,* Volume 35(3), p. 245–296.

Iverson, R. M.; Reid, M. E.; Logan, M.; LaHusen, R. G.; Godt, J. W.; Griswold, J. P., 2011. Positive feedback and momentum growth during debris-flow entrainment of wet bed sediment. *Nature Geoscience,* Volume 4(2), pp. 116-121.

Jakob, M. & Hungr, O., 2005. Debris-Flows Hazard and Related Phenomena. In: Berlin: Springer, pp. pp. 9-24.

Jakob, M., Stein, D. & Ulmi, M., 2012. Vulnerability of buildings to debris flow impact. *Natural hazards,* Volume 60, pp. 241-261.

Jhonson, A. M. & Rodine, J. R., 1984. Debris flow. In: *Slope Instability.* England: Jhon Wile & Sons Ltd., p. pp. 257–361.

Li, J.; Chen, H.; Xu, C. Y.; Zhao, H.; Huo, R.; Chen, J., 2022. Joint Effects of the DEM Resolution and the Computational Cell Size on the Routing Methods in Hydrological Modelling. *Water,* Volume 14(5), p. 797.

MacLaughlin, M., Sitar, N., Doolin, D. & Abbot, T., 2001. Investigation of slope-stability kinematics using discontinuous deformation analysis. *International Journal of Rock Mechanics and Mining Sciences,* Volume 38(5), pp. 753-762.

Martínez-Aranda, S., Murillo, J. & García-Navarro, P., 2022. A GPU-accelerated Efficient Simulation Tool (EST) for 2D variable-density mud/debris flows over non-uniform erodible beds. *Engineering Geology,* Volume 296, p. 106462.

Medina Iglesias, V., 2011. *Debris flows and general steep slope shallow water flows numerical simulation,* Barcelona: Universitat Politècnica de Catalunya (UPC).

Medina, E.; García, H.; Machuca, S.; Medina, D.; Rangel, M.; Sandoval, A.; Morales, J.; Barrera, L.; Gamboa, C.; Ruiz, GL., 2017. *Caracterización del movimiento en masa tipo flujo del 31 de marzo de 2017 en Mocoa, Putumayo,* s.l.: Servicio Geológico Colombiano, Ministerio de Minas y Energía, República de Colombia.

Medina, V., Hürlimann, M. & Bateman, A., 2008. Application of FLATModel, a 2d finite volume code, to debris flows in the northeastern part of the Iberian peninsula. *Landslides,* Volume 5(1), p. 127–142.

Naef, D., Rickenmann, D., Rutschmann, P. & McArdell, B. W., 2006. Comparison of flow resistance relations for debris flows using a one-dimensional finite element simulation model. *Natural Hazards and Earth System Sciences,* Volume 6(1), pp. 155-165.

Núñez-Andrés, M. A., Buill, F., Hürlimann, M. & Abancó, C., 2019. Multi-temporal analysis of morphologic changes applying geomatic techniques 70 years of torrential activity in the Rebaixader catchment (Central pyrenees). *Geomatics, Natural Hazards and Risk,* Volume 10(1), pp. 314-335.

Papa, M. N., Sarno, L., Vitiello, F. S. & Medina, V., 2018. Application of the 2D depth-averaged model, FLATModel, to pumiceous debris flows in the Amalfi Coast. *Water,* Volume 10(9), p. 1159.

Pasculli, A., Cinosi, J., Turconi, L. & Sciarra, N., 2021. Learning case study of a shallow-water model to assess an early-warning system for fast alpine muddy-debris-flow. *Water,* Volume 13(6), p. 750.

Pirulli, M., 2010. On the use of the calibration-based approach for debris-flow forward-analyses. *Natural Hazards and Earth System Sciences,* Volume 10(5), pp. 1009-1019.

Pontificia Universidad Javeriana, 2017. *Consultoría de los estudios de diseño del sistema de alerta temprana para avenidas torrenciales y crecientes súbitas generadas por precipitaciones de la microcuenca de los ríos Mulato, Sangoyaco, quebradas Taruca y Taruquita del municipio de Mocoa,* s.l.: Unidad Nacional para la Gestión del Riesgo de Desastres (UN-GRID).

Portilla, M., Chevalier, G. & Hürlimann, M., 2010. Description and analysis of the debris flows occurred during 2008 in the Eastern Pyrenees. *Natural hazards and Earth system sciences,* Volume 10(7), p. Natural hazards and Earth system sciences.

Prada-Sarmiento, L. F.; Cabrera, M. A.; Camacho, R.; Estrada, N.; Ramos-Cañón, A. M., 2019. The Mocoa Event on March 31 (2017): analysis of a series of mass movements in a tropical environment of the Andean-Amazonian Piedmont. *Landslides,* Volume 16, pp. 2459-2468.

Rickenmann, D., Laigle, D., McArdell, B. & Hubl, J., 2006. Comparison of 2d debris-flow simulation models with field events. *Computational Geosciences,* Volume 10(2), p. 241–264.

Ruiz, G. L.; Reyes, A.; Medina, E.; Sandoval, A.; García, H.; Morales, J. C.; Pérez, M. A.; Gamboa, C. A.; Barrera, L. A., 2018. *Amenaza por movimientos en masa tipo flujo en las cuencas de las quebradas Taruca, Taruquita, San Antonio y El Carmen y los ríos Mulato y Sangoyaco, municipio de Mocoa - Putumayo, Escala 1:5.000,* s.l.: Servicio Geológico Colombiano, Ministerio de Minas y Energía, República de Colombia.

Saleem, N.; Huq, M. E.; Twumasi, N. Y. D.; Javed, A.; Sajjad, A., 2019. Parameters derived from and/or used with digital elevation models (DEMs) for landslide susceptibility mapping and landslide risk assessment: a review. *ISPRS International Journal of Geo-Information,* Volume 8(12), p. 545.

Stancanelli, L. M. & Foti, E., 2015. A comparative assessment of two different debris flow propagation approaches–blind simulations on a real debris flow event. *Natural Hazards and Earth System Sciences,* Volume 15(4), pp. 735-746.

Takebayashi, H. & Fujita, M., 2020. Numerical simulation of a debris flow on the basis of a two-dimensional continuum body model. *Geosciences,* Volume 10(2), p. 45.

Wang, B., Li, Y., Liu, D. & Liu, J., 2018. Debris flow density determined by grain composition. *Landslides,* Volume 15, pp. 1205-1213.

Yong, L.; Xiaojun, Z.; Pengcheng, S.; Yingde, K.; Jingjing, L., 2013. A scaling distribution for grain composition of debris flow. *Geomorphology,* Volume 192, pp. 30-42.

Annexes

Figure 25. Flow depth map of 2017 debris flow event in Mocoa (Medina, et al., 2017).

Table 5. Comparison of the discharge modeled (FLO2D) and empirical results with the methods Wudu and Chezy. The sections are placed in Taruca(Tc) and Taruquita creeks (Tq), and Mulato River (Mt) (Ruiz, et al., 2018).

METHOD	SECTIONS Medina, et al., (2017)	SECTIONS Ruiz, et al., (2018)	FLO2D	EMPIRICAL RESULTS		TERRAIN DISTANCE (m)
			Q (m3/s)	Q (m3/s)	U (m/s)	
Wudu	Tc1	Tc1-5	55.66	2920.7	17.4	680
	Tc1b	Tc1b-4		1931.3	18.5	1200
	Tc2	Tc2-3	110	1238.7	10.8	1900
	Tc3	Tc3-6		2425.8	11.6	2250
	Tc3b	Tc3b-7		1652.1	11	2750
	Tc4	Tc4-8		1312.3	9.4	2990
	Tc5	Tc5-9	362	913.9	9.2	3500
	Tq1	Tq1-1	165	473.7	5.9	2100
	Tq2	Tq2-2	222	355.6	6.1	2400
	Mt1	Mt1-12		236.4	5.6	10600
	Mt2	Mt2-13		700.1	5.5	11000
Chezy	Tc1	Tc1-5	108	1976.4	11.8	680
	Tc1b	Tc1b-4		1391.7	13.3	1200
	Tc2	Tc2-3		1365.9	11.9	1900
	Tc3	Tc3-6	390	2986.7	14.2	2250
	Tc3b	Tc3b-7		2093.1	14	2750
	Tc4	Tc4-8		1274.2	9.2	2990
	Tc5	Tc5-9		909.5	9.1	3500
	Tq1	Tq1-1		588.6	7.4	2100
	Tq2	Tq2-2		416.6	7.2	2400
	Mt1	Mt1-12	137	388.1	9.2	10600
	Mt2	Mt2-13	217	1099.8	8.6	11000